Journal of Mathematical Chemistry Vol. 30, No. 1, July 2001 (© 2001)

Boundary effects in the hexagonal packing of rod-like molecules inside a right circular cylindrical domain. III. The case of arbitrarily oriented spherocylindrical molecules

A.F. Antippa [a], J.-J. Max [b] and C. Chapados [b]

[a] *Département de Physique, Université du Québec à Trois-Rivières Trois-Rivières, Québec, Canada G9A 5H7*

[b] *Département de Chimie-Biologie, Université du Québec à Trois-Rivières Trois-Rivières, Québec, Canada G9A 5H7*

Received 25 April 2001

We study the organization of spherocylindrical molecules inside a freely rotating right circular cylindrical domain at the gas/liquid interface. The analysis is made under the assumption that the molecules are rigid and close packed, and that they are oriented parallel to each other. The direction and angle of their common orientation are completely arbitrary. We obtain exact analytic expressions for the lattice of molecular centers and its boundaries as a function of molecular dimensions, molecular orientation, and domain size. As a first application, we derive the number of molecules in a domain, and the packing fraction. The results obtained are essential when attempting to analytically model a Langmuir film where the global order of the film is less than the local order of the domains.

KEY WORDS: molecular, organization, Langmuir, films, gas, liquid, interface, boundary effects, hexagonal, packing, orientation, spherocylindrical, rod-like, molecules

1. Introduction

In this paper (as in [1,2]), we are concerned with the theoretical modeling of the molecular organization of Langmuir films at the gas/liquid interface. Specifically we study the close packing of spherocylindrical molecules inside a right circular cylindrical freely rotating domain whose axis is perpendicular to the interface. By treating the problem at two scales simultaneously we are able to account for boundary effects. We obtain exact analytic expressions for the lattice of molecular centers and its boundaries as a function of molecular dimensions, molecular orientation, and domain size. As a first application of this structural study, we evaluate the packing fraction as a function of the size of the domain, the size of the molecules, and the orientation of the molecular axes.

Experimentally, monolayers of amphiphilic molecules at the air/water interface show some characteristic patterns even when simple lipids are used [3]. When mono-

0259-9791/01/0700-0031$19.50/0

layers are transferred onto plates Langmuir–Blodgett films are obtained. One to several layers can be deposited by this technique. Experimentally, periodic structures are observed in lipid monolayers when, in order to study pattern organization, low concentration fluorescent probes are introduced in the lipid films [4,5]. These patterns influence the formation of micelles, vesicles, liposomes, membranes, and Langmuir–Blodgett films [3]. X-ray diffraction and scanning probe microscopy also reveal pattern organization in these mono- and multi-layers [6,7], and Brewster angle microscopy on Langmuir films is used to study the domain morphology [8,9]. In phospholipid bilayers some patterns are observed using atomic force microscopy [10,11]. A good review of the subject is given by McConnell [12].

The first step in the study of the organization of bilayers, multilayers, liposomes, etc. is the study of the organization of the monolayer film. This study can be separated into two parts: structural organization and dynamics. Organization mainly depends on molecular dimensions and orientation. Dynamics mainly depends on the Van der Waals interactions between the aliphatic chains, and the electrostatic interactions between the polar heads and the liquid phase. Due to the complexity of the problem, we have chosen to study the above two parts sequentially.

In the first article on structural organization, we studied the case of spherocylindrical molecules aligned vertically [1]. The boundary effects, in as far as the domain density is concerned, were found to be non-negligible (about 2.5%) for domains containing less than 10,000 molecules and as high as 20% for small domains. This first article allowed us to clarify the physical basis of the model, to introduce the appropriate notation, and to develop the mathematical techniques needed in packing inside a cylindrical domain. We exploited the hexagonal symmetry, present in the case of vertically aligned molecules, in order to define the coordinate axes, and the half-way plane. We also defined the reference lattice formed by the intersection of the molecular axes of the vertically aligned molecules with the half-way plane. Most important, from this study we learned how to handle the two-dimensional boundary problem of packing circular molecular cross-sections inside a circular domain cross-section.

The second article in the series dealt with inclined spherocylindrical molecules tilted toward next nearest neighbors [2]. The importance of boundary effects was found (as expected) to increase rapidly with the angle of inclination and length of the molecules. The case of tilted molecules lead to a packing problem that is irreducibly three-dimensional, and we used projective geometry to determine the boundaries of the lattice formed by the centers of the molecules of the domain. The complexity of the problem in the case of inclined molecules forced us to restrict the analysis to only one specific direction of inclination.

In this third paper of the series, we study the general case of arbitrarily oriented molecules aligned parallel to each other and inscribed within a right circular cylindrical domain. The solution, as presented here, is essential when attempting to model a Langmuir film. The film is built up of a distribution of domains with variable molecular orientations, and the structure of the distribution function determines the ratio of the degree of global order (at the film scale) to the degree of intermediate order (at the

domain scale). The handling of this general problem has been greatly simplified by the progressive solution of its various facets in the two preceding articles of the series, and by the introduction of the tilting operator [13], which transforms the initial reference lattice (lattice of the centers of vertically aligned molecules) into the lattice of the centers of arbitrarily oriented molecules. The application of the tilting operator to the reference lattice of hexagonally packed molecules constitutes the starting point of the present work.

We will use three-dimensional graphic simulations (a virtual-reality representation of the domain) to complement the analytic algebraic results. These graphic simulations provide an instant independent visual verification of the mathematical results obtained.

2. The model

We will only give a summary of the essential features of the underlying model and refer the reader to [1,2,13] for details and justification. Globally the system we are dealing with presupposes phospholipidic molecules arranged in domains forming a Langmuir film at the gas/liquid interface. The molecules of the domain are embedded in identical "virtual" spherocylindrical [14] (rod-like [15]) molecules that are aligned parallel to each other. It is assumed that as the molecules are inclined they slide along each other (obliquely) in order for their polar heads to remain tangent to a plane parallel to the interface. That is, we assume hydrodominance [13].

2.1. The molecules

The spherocylindrical molecule is shown in figure 1. The molecular cylinder has radius r_0 and height h. The molecular hemispheres have radius r_0. The total length d of the molecule is given by $d = h + 2r_0$. The molecules are assumed to be all identical and aligned parallel to each other. Their collective orientation is given by the spherical angles θ and ϕ, with the z-axis in the direction of the normal to the interface.

2.2. The domain

We refer to the above assembly of parallel molecules as the "*physical domain*". The "*virtual domain*" is a right circular cylinder enveloping the molecules of the "physical domain" as shown in figure 2. The axis of this circumscribing cylinder is perpendicular to the gas/liquid interface. Its radius R and height H are determined by the condition that R and H be as small as possible. The height H depends on the inclination of the molecules relative to the interface, and is given by $H(r_0, h, \theta) = 2r_0 + h\cos\theta$. The radius R is equal to half the largest dimension of the projection of the "physical domain" on the interface. Its value is a function of the number of molecules in the domain, the dimensions of these molecules, and their angle and direction of inclination. The word domain, without qualification, will throughout the paper denote the virtual cylindrical circumscribing domain.

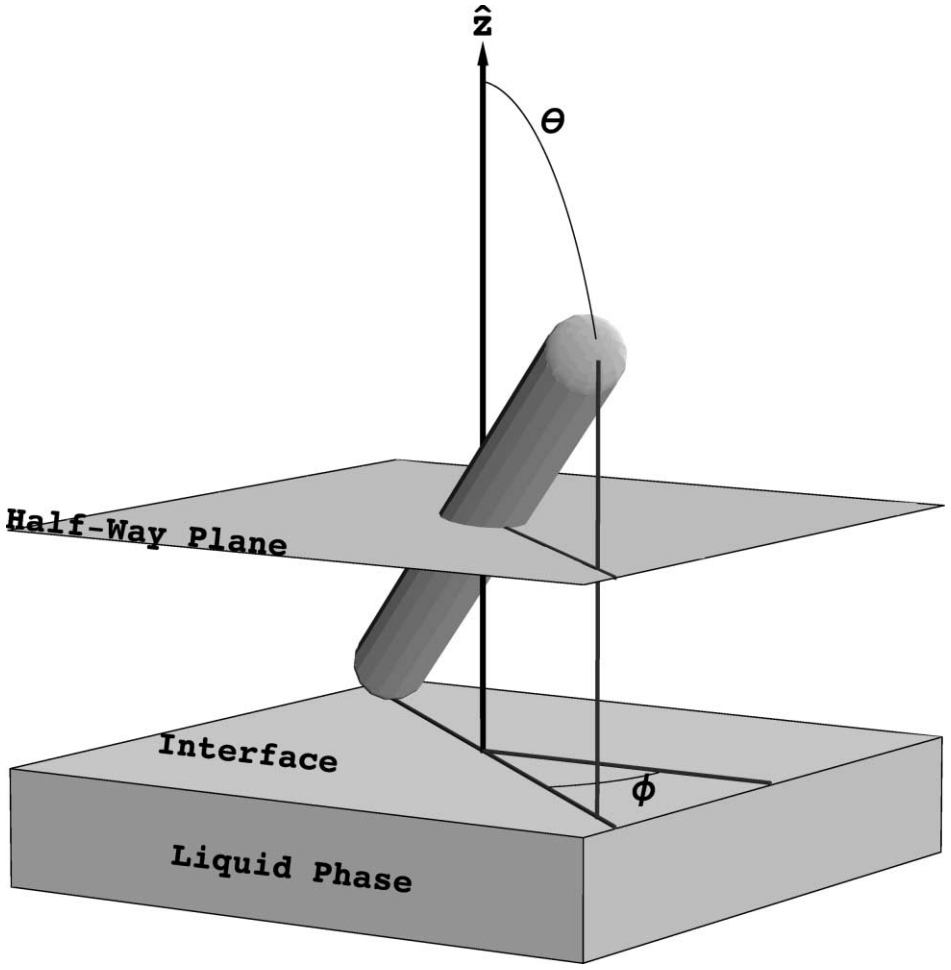

Figure 1. Spherocylindrical molecule at the gas/liquid interface. The half-way plane is parallel to the interface and passes through the center of symmetry of the molecule. The molecule is tilted by an angle θ with respect to the normal to the interface. The direction of tilting is ϕ.

2.3. The half-way plane

The plane perpendicular to the symmetry axis of the virtual domain and situated half-way in-between the base and the top is referred to as the *half-way plane*. The points of intersection of the molecular axes with the half-way plane (the centers of the molecules) define a two-dimensional lattice in this plane (see figure 3). The cross-section of the virtual domain in the half-way plane is a disc of radius R. The symmetry axis of the virtual domain passes through the center of this disc. The projection of the physical domain on the half-way plane possesses reflection symmetry through this center. This reflection symmetry is unique to the half-way plane, and is the main reason for choosing to work in it rather than in the plane of the interface.

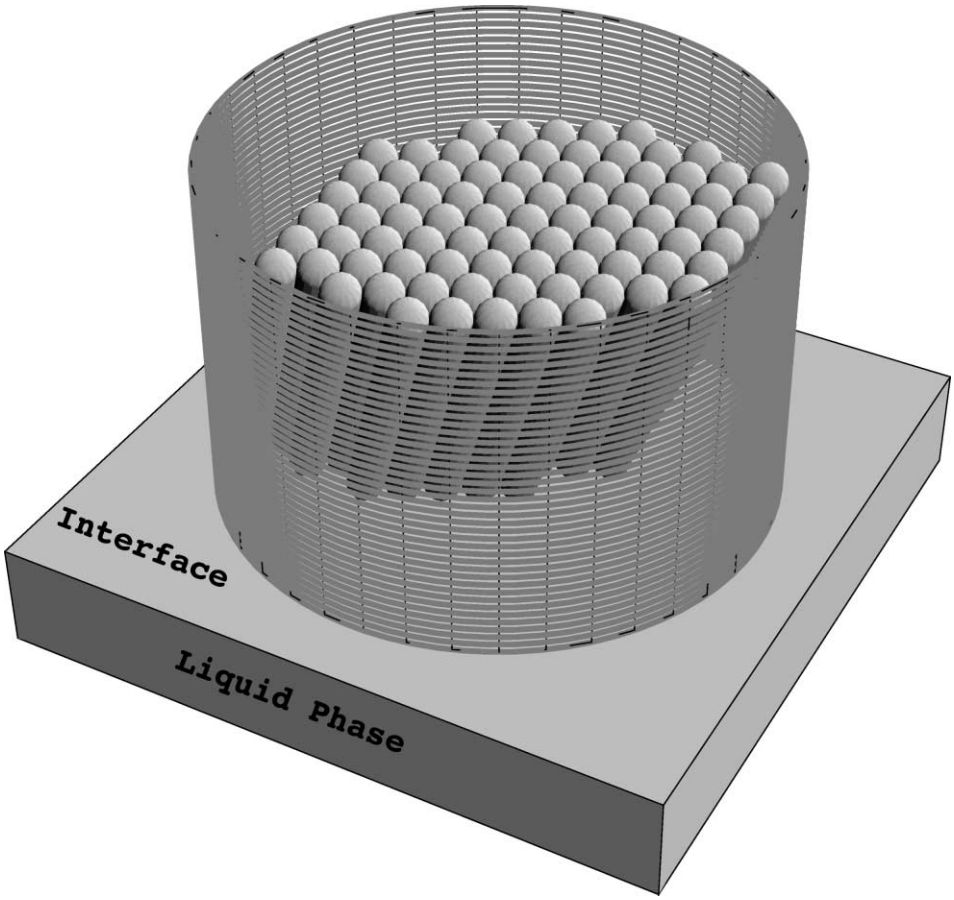

Figure 2. The physical domain of parallel spherocylindrical molecules having an arbitrary collective orientation is confined within a virtual cylindrical domain. The parameters used in generating the figure are $R/r_0 = 15$, $h/r_0 = 20$, $\theta = \pi/6$, and $\phi = -\pi/4$. The resulting domain radius is $R_{\min}/r_0 = 14.9796$, the number of molecules is $N = 83$, and the packing fraction is $\beta = 0.40843$. For very large domains, the domain is essentially a thin disc.

2.4. The reference lattice

When the molecules of the physical domain are vertically oriented we refer to the lattice of the centers of the molecules as the "*reference lattice*". In the case of vertically oriented molecules, the optimal packing of spherocylindrical (rod-like) molecules in a cylindrical domain is hexagonal [1], and consequently, the reference lattice has three principal and three secondary axes of symmetry as shown in figure 4. The high degree of symmetry in the case of vertically aligned molecules simplifies the process of introducing and defining a *system of axes*.

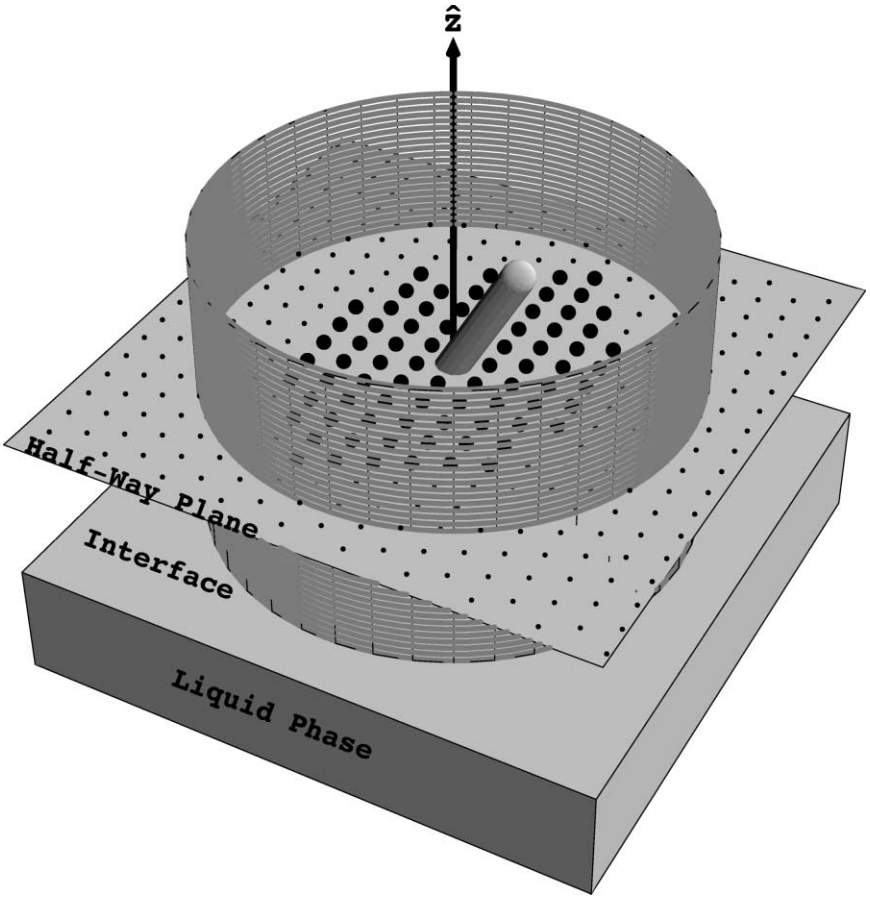

Figure 3. The lattice (in the half-way plane) formed by the centers of the molecules of the domain. The occupied lattice sites (corresponding to the centers of the molecules that are confined in the domain) are indicated by dark disks. The parameters used in generating the figure are $R/r_0 = 15$, $h/r_0 = 20$, $\theta = \pi/6$, and $\phi = -\pi/12$. The resulting domain radius is $R_{\min}/r_0 = 14.9796$, the number of molecules is $N = 83$, and the packing fraction is $\beta = 0.40843$.

2.5. The coordinate systems

Using the symmetry axes of the reference lattice, we introduce three coordinate systems as shown in figure 5. The first is the $(\hat{x}, \hat{y}, \hat{z})$ coordinate system which is fixed to the half-way plane, and defined as follows: (i) the *z-axis* coincides with the axis of the circumscribing cylinder, (it is normal to the interface); (ii) the intersection of the z-axis with the half-way plane defines the *origin* of coordinates; (iii) the *xy plane* coincides with the half-way plane; (iv) the x-axis coincides with one of the secondary axes of symmetry; (v) the y-axis coincides with one of the principal axes of symmetry. Due to the hexagonal symmetry of the reference lattice, the above system of coordinates is orthogonal. As the molecules are tilted, the half-way plane moves relative to the interface and this $(\hat{x}, \hat{y}, \hat{z})$ coordinate system moves with it.

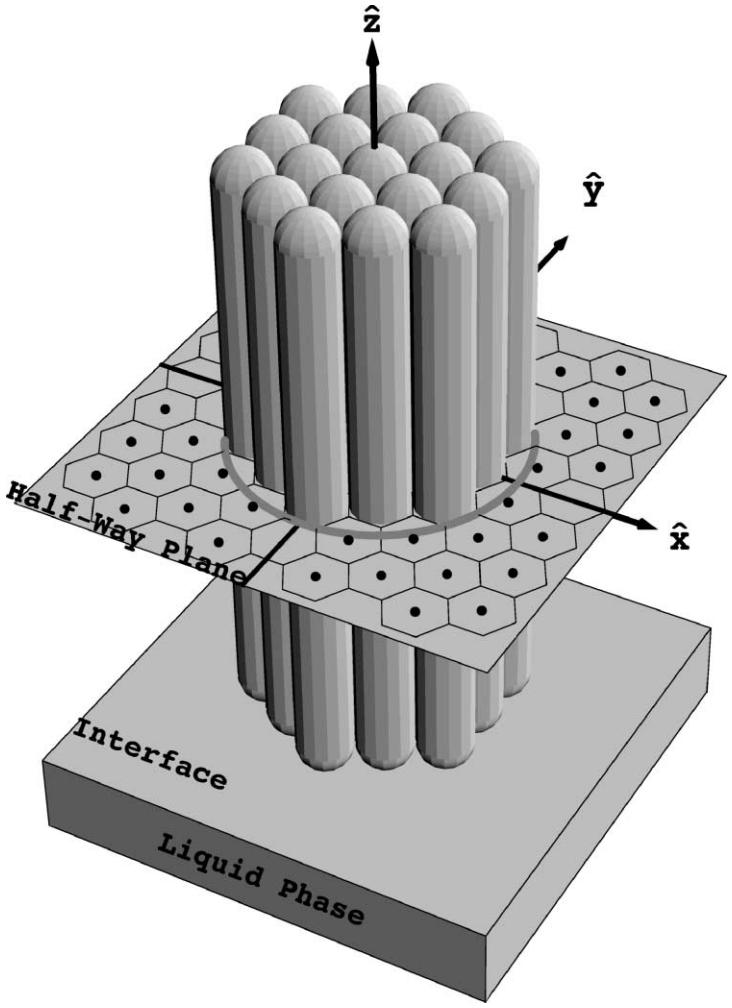

Figure 4. The "reference" lattice of vertically oriented molecules serves to define the system of axes. The origin is at the center of the central molecule. The z-axis is in the direction of the normal to the interface. The y-axis is in the direction of a principal axis of symmetry. The x-axis is in the direction of a secondary axis of symmetry. Hexagonal symmetry guaranties that the system of axes is orthogonal. The parameters used in generating the figure are $R/r_0 = 6$, $h/r_0 = 20$, $\theta = 0$, and $\phi = 0$. The resulting domain radius is $R_{\min}/r_0 = 5$, the number of molecules is $N = 19$, and the packing fraction is $\beta = 0.73697$.

Next we introduce the $(\hat{m}, \hat{n}, \hat{z})$ coordinate system, which is also fixed to the half-way plane. It is obtained from the $(\hat{x}, \hat{y}, \hat{z})$ coordinate system by a rotation ϕ about the $\hat{z}$-axis. Hence,

$$\begin{pmatrix} \hat{m} \\ \hat{n} \end{pmatrix} = \begin{pmatrix} \cos\phi & \sin\phi \\ -\sin\phi & \cos\phi \end{pmatrix} \begin{pmatrix} \hat{i} \\ \hat{j} \end{pmatrix}, \tag{1}$$

where $\hat{i}$ and $\hat{j}$ are unit vectors along $\hat{x}$ and $\hat{y}$, respectively.

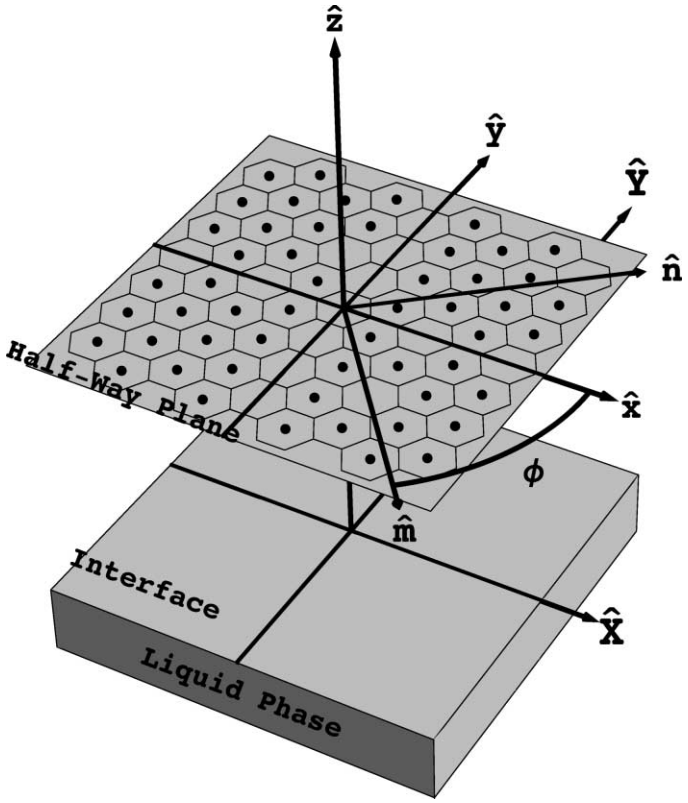

Figure 5. The three systems of coordinates. The $(\hat{x}, \hat{y}, \hat{z})$ coordinate system is as defined in figure 4 and is fixed to the half-way plane. The $(\hat{m}, \hat{n}, \hat{z})$ coordinate system is obtained from the $(\hat{x}, \hat{y}, \hat{z})$ coordinate system by a rotation of angle ϕ about the $\hat{z}$ axis. The $(\widehat{X}, \widehat{Y}, \widehat{Z})$ coordinate system is "fixed in space". It's origin is on the interface. Its axes are parallel to the $(\hat{x}, \hat{y}, \hat{z})$ axes. Its $\widehat{Z}$-axis coincides with the $\hat{z}$-axis. The lattice is that of vertically oriented molecules. The parameters used in generating the figure are $h/r_0 = 20$, $\theta = 0$, and $\phi = -50°$.

Finally, we introduce the space-fixed coordinate system $(\widehat{X}, \widehat{Y}, \widehat{Z})$ which is attached to the interface. Its origin is on the interface. Its $\widehat{Z}$-axis is collinear with the $\hat{z}$-axis. Its $\widehat{X}\widehat{Y}$ plane coincides with the interface, and its $\widehat{X}$- and $\widehat{Y}$-axes parallel to $\hat{x}$ and $\hat{y}$, respectively. Hence, the $(\widehat{X}, \widehat{Y}, \widehat{Z})$ and $(\hat{x}, \hat{y}, \hat{z})$ coordinate systems are related by the vertical translation

$$\{\vec{X}, \vec{Y}, \vec{Z}\} = \left\{\vec{x}, \vec{y}, \left(z + r_0 + \frac{h}{2}\cos\theta\right)\hat{z}\right\}. \tag{2}$$

2.6. The lattice of arbitrarily oriented molecules

Relative to the above defined reference frames, the intersection of the molecular axes with the half-way plane produces a lattice whose sites are given by [13, equation (25b)]

$$\vec{r}_{\ell k}(\theta,\phi) = \hat{i} r_0 \{\ell\sqrt{3}(\sin^2\phi + \sec\theta\cos^2\phi) + (2k-\ell)(\sec\theta - 1)\sin\phi\cos\phi\} + \hat{j} r_0 \{(2k-\ell)(\sec\theta\sin^2\phi + \cos^2\phi) + \ell\sqrt{3}(\sec\theta - 1)\sin\phi\cos\phi\}, \tag{3}$$

where ℓ and k are integers, θ is the tilting angle (the angle that the molecular axes make with the normal to the interface), and ϕ determines the tilting plane (the plane defined by the molecular axis and a normal to the interface). The length of vector (3) is

$$r_{\ell k}(\theta,\phi) = r_0\sqrt{4(\ell^2 + k^2 - k\ell) + \left[\sqrt{3}\ell\cos\phi + (2k-\ell)\sin\phi\right]^2\tan^2\theta}. \tag{4}$$

2.7. Auxiliary conditions

2.7.1. Restrictions on the angle of inclination

Since the molecules of the domain cannot be inclined at more than $\pi/2$ without being fully submerged in the liquid phase, then the range of θ is restricted to $0 \leqslant \theta \leqslant \pi/2$. Furthermore, we require that the domain radius be large enough to accommodate at least one molecule tilted at θ degrees to the normal. Combining these two conditions, we find that the range of θ is restricted to

$$0 \leqslant \theta \leqslant \arcsin\left[2\left(\frac{R - r_0}{h}\right)\right]. \tag{5}$$

Constraint (5) is a physical "steric" constraint. It must always be satisfied, and will be assumed to hold throughout the analysis.

2.7.2. Symmetries of the direction of inclination

Due to the symmetry of the spherocylindrical molecule, its projection on the halfway plane is invariant under a rotation of π radians. Furthermore, the reference lattice (the lattice of the vertically aligned molecules) is the starting point for tilting, and, due to its hexagonal symmetry, all non-equivalent tilting orientations can be reached by restricting the angle ϕ to a range of $\pi/3$. Specifically, we can take this range to be $0 \leqslant \phi \leqslant \pi/3$. In this range $\sin\phi \geqslant 0$, and $(\sqrt{3}\cos\phi - \sin\phi) \geqslant 0$. The constraints on ϕ are dependent on the exact symmetry of the spherocylindrical molecule, as well as the exact hexagonal symmetry of the reference lattice. Hence, even though they simplify the analysis, we will not make use of them in order not to irremediably restrict the validity of the resulting expressions. Nonetheless, we expect this symmetry to manifest itself in the resulting equations of the present paper.

3. The occupied lattice sites

Equation (3) gives the lattice sites through which a molecular axis can potentially pass, but it does not guarantee that the corresponding molecule is inside the domain. In this section we will determine the values of (ℓ, k) for which the corresponding molecule

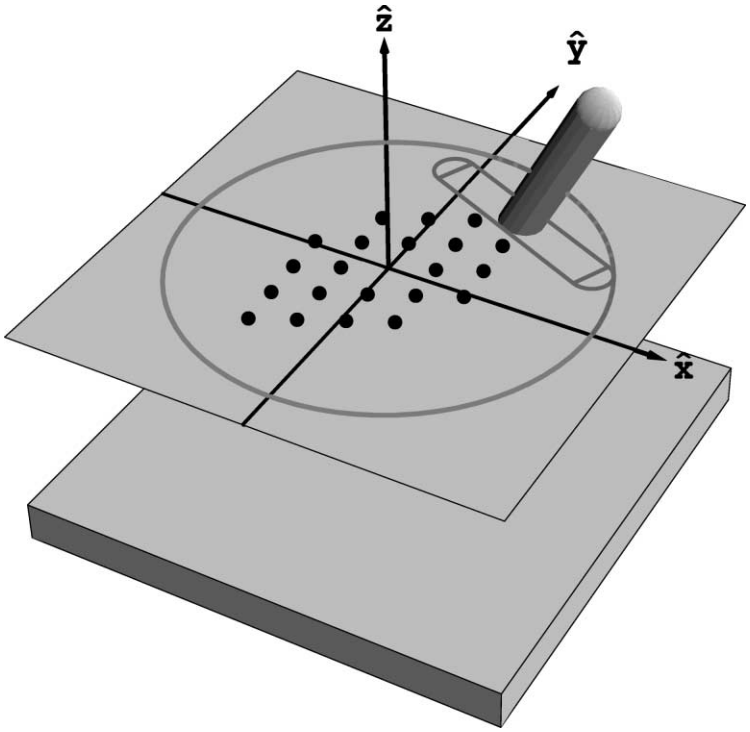

Figure 6. The furthest molecule and its projection on the half-way plane. Also shown is the lattice (in the half-way plane) formed by the centers of the molecules of the domain. The occupied lattice sites (corresponding to the centers of molecules confined in the domain) are indicated by dark disks. The parameters used in generating the figure are $R/r_0 = 10$, $h/r_0 = 20$, $\theta = 30°$, and $\phi = -25°$. The resulting domain radius is $R_{\min}/r_0 = 9.94952$, the number of molecules is $N = 23$, and the packing fraction is $\beta = 0.25654$.

is inside the domain. That is, we determine the occupied lattice sites. Since the axis of the virtual domain is perpendicular to the gas/liquid interface, then a molecule will be totally inscribed in the virtual domain if, and only if, its projection on the half-way plane is totally inscribed in the circle formed by the intersection of the virtual domain with the half-way plane. Thus, by using projections, we reduce the three-dimensional problem of inscribing molecules in a cylinder, into a two-dimensional problem of inscribing molecular projections inside a circle, as shown in figure 6.

3.1. Parameterizing the projection

The molecular projection on the half-way plane is divided into four segments, as shown in figure 7. The two half-circles s_1 and s_2 and the two straight lines s_3 and s_4. The center of symmetry of the molecular projection on the half way plane is designated by c_0 and situated at a lattice site. The vector from the origin of coordinates to c_0 is $\vec{r}_{\ell k}(\theta, \phi)$ as given by equation (3). The centers of the two half-circles (boundaries of the projection of the hemispherical parts of the molecule) are designated by c_1 and c_2. The mid-points

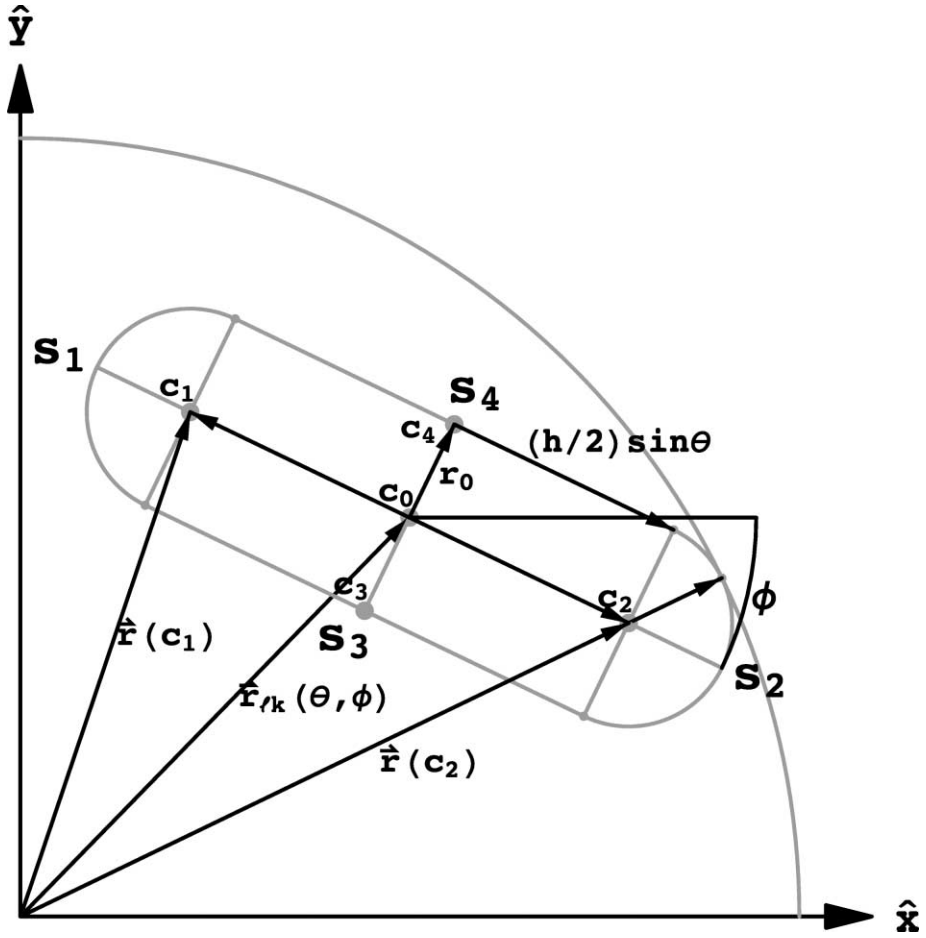

Figure 7. The projection of a molecule on the half-way plane is divided into four segments: two half-circles s_1 and s_2 and the two straight lines s_3 and s_4. The center of symmetry of the molecular projection is c_0. The vector from the origin to c_0 is $\vec{r}_{\ell k}(\theta, \phi)$. The centers of the two half-circles are c_1 and c_2. The mid-points of the two straight segments are c_3 and c_4. The vectors from the origin to c_q ($q = 0, 1, 2, 3, 4$) are designated by $\vec{r}(c_q)$. The parameters used in generating the figure are $r_0 = 1.25$, $R = 8$, $h = 10$, $\theta = \pi/5$, and $\phi = -\pi/7$. The coordinates of the center of the molecular projection are given via equation (3) by $\ell = 2$ and $k = 3$.

of the two straight segments (boundaries of the projection of the cylindrical part of the molecule) are designated by c_3 and c_4. The vectors from the origin of coordinates to c_q ($q = 0, 1, 2, 3, 4$) will be designated by $\vec{r}(c_q)$. The vectors $\overrightarrow{c_0 c_q}$ from c_0 to c_q are given by

$$\overrightarrow{c_0 c_q} = \begin{cases} (-1)^q \dfrac{h \sin\theta}{2} \hat{m} & \text{for } q = 1, 2, \\ (-1)^q r_0 \hat{n} & \text{for } q = 3, 4, \end{cases} \tag{6}$$

where $\hat{m}$ and $\hat{n}$ are given by equation (1). Since

$$\vec{r}(c_q) = \vec{r}_{\ell k}(\theta, \phi) + \overrightarrow{c_0 c_q}, \quad q = 0, 1, 2, 3, 4, \tag{7}$$

then, making use of equations (3) and (6), this can be written out explicitly as

$$\begin{aligned}\vec{r}(c_q) = \hat{i} r_0 \Big\{ & \ell\sqrt{3}\big(\sin^2\phi + \sec\theta\cos^2\phi\big) + (2k-\ell)(\sec\theta - 1)\sin\phi\cos\phi \\ & + (-1)^q \frac{h}{2r_0}\sin\theta\cos\phi \Big\} \\ + \hat{j} r_0 \Big\{ & (2k-\ell)\big(\sec\theta\sin^2\phi + \cos^2\phi\big) + \ell\sqrt{3}(\sec\theta - 1)\sin\phi\cos\phi \\ & + (-1)^q \frac{h}{2r_0}\sin\theta\sin\phi \Big\}, \quad q = 1, 2,\end{aligned} \tag{8a}$$

and

$$\begin{aligned}\vec{r}(c_q) = \hat{i} r_0 \big\{ & \ell\sqrt{3}\big(\sin^2\phi + \sec\theta\cos^2\phi\big) + (2k-\ell)(\sec\theta - 1)\sin\phi\cos\phi \\ & - (-1)^q \sin\theta \big\} \\ + \hat{j} r_0 \big\{ & (2k-\ell)\big(\sec\theta\sin^2\phi + \cos^2\phi\big) + \ell\sqrt{3}(\sec\theta - 1)\sin\phi\cos\phi \\ & + (-1)^q \cos\theta \big\}, \quad q = 3, 4.\end{aligned} \tag{8b}$$

To continue with the paramatrization we designate by $\vec{r}(P) = (x(P), y(P))$ the vector from the origin of coordinates to a point P on the perimeter of the projection (on the half-way plane) of the molecule whose center is at $\vec{r}_{\ell k}(\theta, \phi)$. The coordinates of P are given by

$$\vec{r}(P) = \begin{cases} \vec{r}(c_q) + r_0 \hat{e}(P) & \text{for } q = 1, 2, \\ \vec{r}(c_q) + \hat{m}\xi & \text{for } q = 3, 4, \end{cases} \tag{9}$$

where $\hat{e}(P)$ is a unit vector in the direction $\overrightarrow{c_q P}$, and ξ is restricted to the range $-(h/2)\sin\theta \leqslant \xi \leqslant (h/2)\sin\theta$.

3.2. The furthest point of a molecular projection

In this section we want to determine the radius vector $\vec{r}_{\max} \equiv \vec{r}(P_{\max})$ from the origin (center of the virtual domain) to the furthest point $P_{\max}$ of the projection of the molecule on the half-way plane. We proceed in three steps:

(i) First we prove that the furthest point is on one of the two half-circles.

(ii) Then we find the furthest point on a half-circle.

(iii) Finally we find the center of the half-circle that is furthest from the origin.

The three results combined determine the point, on the molecular projection, which is furthest from the origin.

3.2.1. The furthest point on a straight segment

The furthest point of the molecular projection necessarily lies on the projection of one of the hemispheres. That is:

$$\max\left\{r(P \in \underbrace{s_1 \cup s_2}_{\substack{\text{projection of}\\ \text{hemispheres}}})\right\} \geqslant \max\left\{r(P \in \underbrace{s_3 \cup s_4}_{\substack{\text{projection of}\\ \text{cylinder}}})\right\}. \tag{10}$$

This result can be proved by showing that the furthest point on a straight segment lies at one of its extremities. In other words, it lies on the intersection of the straight segment (part of the boundary of the projection of the cylindrical part of the molecule) with a half-circle (boundary of the projection of one of the hemispherical parts of the molecule).

The radius vectors to points on the straight segments s_3 and s_4 are given by equation (9). Hence, their lengths are given by

$$\begin{aligned} &r^2(P) = \xi^2 + 2\vec{r}(c_q)\cdot\hat{m}\xi + r^2(c_q),\\ &-\frac{h}{2}\sin\theta \leqslant \xi \leqslant \frac{h}{2}\sin\theta, \quad P \in s_q, \quad q = 3, 4. \end{aligned} \tag{11}$$

Corresponding to every point $P(\xi) \in s_q$ for $q = 3, 4$ we define two points $P_+ \equiv P(\xi_+)$ and $P_- \equiv P(\xi_-)$ corresponding to $\xi_+ = +|\xi|$ and $\xi_- = -|\xi|$, respectively. Then

$$\begin{aligned} &r^2(P_\pm) = |\xi|^2 \pm 2\vec{r}(c_q)\cdot\hat{m}|\xi| + r^2(c_q),\\ &0 \leqslant |\xi| \leqslant \frac{h}{2}\sin\theta, \quad P_\pm \in s_q, \quad q = 3, 4. \end{aligned} \tag{12}$$

As $|\xi|$ varies from zero to $(h/2)\sin\theta$, P_+ and P_- move out from c_q to the extremities of the straight segment s_q (see figure 8). As can be seen from equation (12), the difference between $r^2(P_+)$ and $r^2(P_-)$ is equal to $\vec{r}(c_q)\cdot\hat{m}$ which is constant, and consequently, as $|\xi|$ varies from zero to $(h/2)\sin\theta$, the relation between $r^2(P_+)$ and $r^2(P_-)$ remains invariant. Hence, we can designate by $r^2(P_>)$ the larger of $r^2(P_+)$ and $r^2(P_-)$, or explicitly,

$$r^2(P_>) = |\xi|^2 + 2\left|\vec{r}(c_q)\cdot\hat{m}\right||\xi| + r^2(c_q), \qquad 0 \leqslant |\xi| \leqslant \frac{h}{2}\sin\theta, \quad P_> \in s_3 \cup s_4. \tag{13}$$

The above expression for $r^2(P_>)$ is a monotonically increasing function of $|\xi|$, and takes its maximum value when $|\xi|$ is maximum ($|\xi|_{\max} = (h/2)\sin\theta$). That is, $r^2(P_>)$ is maximum when point $P_>$ is at one of the extremities of either the straight segment s_3 or the straight segment s_4. But every extremity of a straight segment lies on a half-circle (projection of one of the two hemispheres). This completes the proof of equation (10) which states that the furthest point of the molecular projection lies on the projection of one of the two hemispheres.

3.2.2. The furthest point on a half-circle

Having established that the furthest point necessarily lies on the projection of one of the two hemispheres, we now proceed to determine the furthest point on the projection of a hemisphere. Consider a circle in the half-way plane centered at the origin and

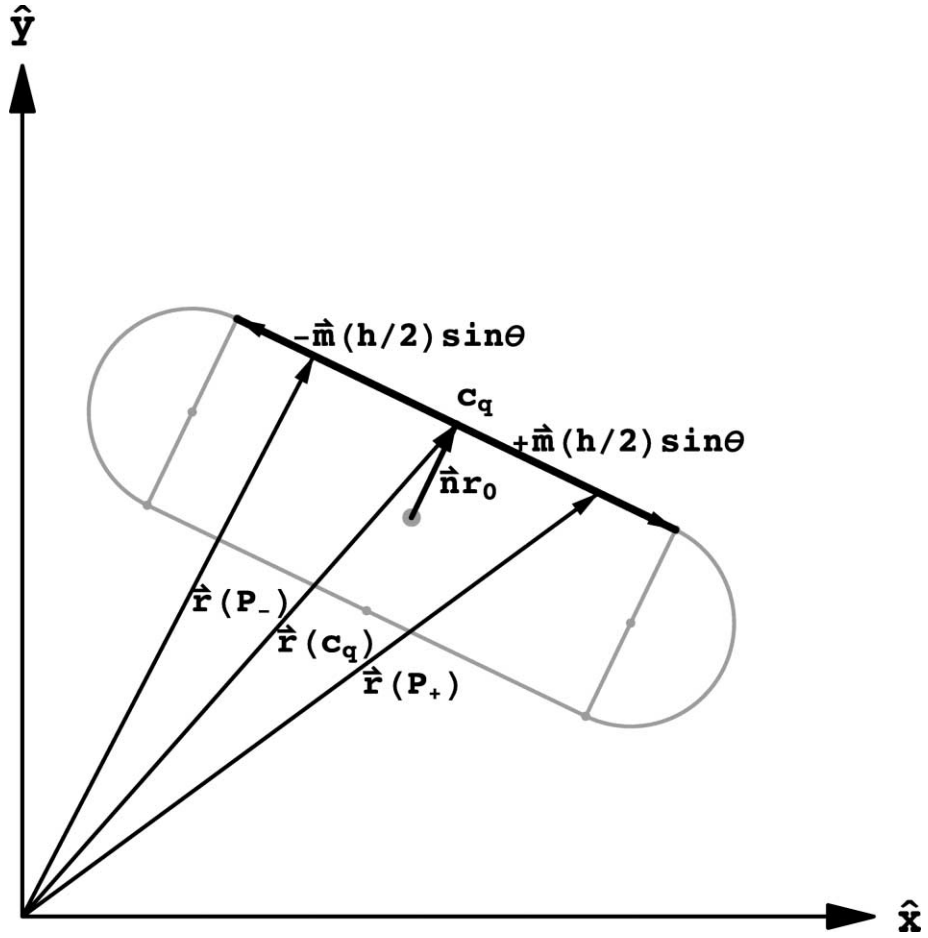

Figure 8. Geometric proof that the furthest point on a straight segment of the molecular projection lies on one of its extremities. That is, it lies on one of the two half-circles. The parameters used in generating the figure are $r_0 = 1.25$, $R = 8$, $h = 10$, $\theta = \pi/5$, and $\phi = -\pi/7$. The coordinates of the center of the molecular projection are given via equation (3) by $\ell = 2$ and $k = 3$.

circumscribing the molecular projection (see figure 9). Since the point $P_{\max}$ (the point, furthest from the origin, on the molecular projection), lies on one of the two half-circular sections s_1 or s_2 (boundaries of the projections of the molecular hemispheres), then the circumscribing circle is tangent, either to s_1 or to s_2, at $P_{\max}$. Hence, if we draw a tangent to the circumscribing circle at $P_{\max}$, this tangent will also be tangent to the inscribed half-circular projection, and the respective radii, from the centers of the inscribed circle and the circumscribing circle, to the point of tangency $P_{\max}$ will both be perpendicular to this tangent, and hence, collinear to each other. In other words, the line from the origin to $P_{\max}$ passes through the center of one of the two half-circles s_1 or s_2. Consequently, the length of the radius vector from the origin to $P_{\max}$ (the furthest point of the molecular projection) is given by

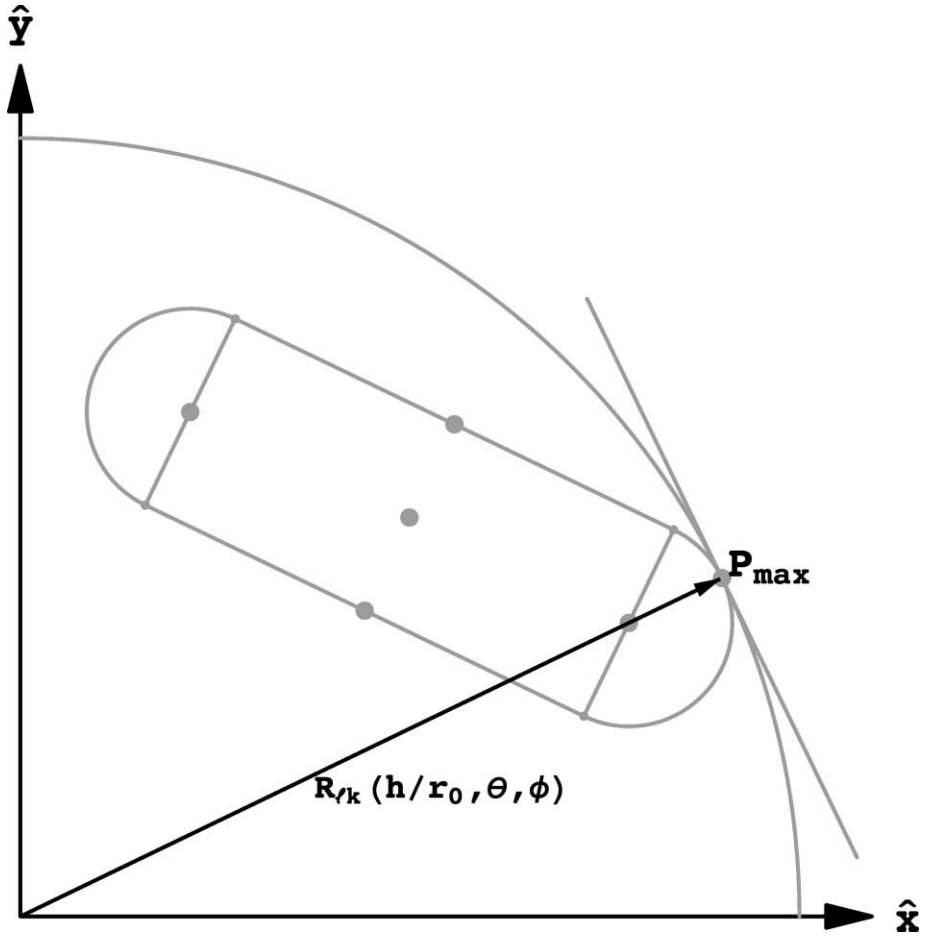

Figure 9. Geometric proof that the line from the origin to the furthest point passes through the center of one of the two half-circles. The parameters used in generating the figure are $r_0 = 1.25$, $R = 8$, $h = 10$, $\theta = \pi/5$, and $\phi = -\pi/7$. The coordinates of the center of the molecular projection are given via equation (3) by $\ell = 2$ and $k = 3$.

$$r_{\max} \equiv r(P_{\max}) = \max\left\{r(c_1), r(c_2)\right\} + r_0. \tag{14}$$

The problem of determining the furthest point on a molecular projection has been reduced to that of determining the larger of the two radius vectors $\vec{r}(c_1)$ and $\vec{r}(c_2)$, from the origin to c_1 and c_2, respectively. That is determining the furthest (from the origin) of the projections of the centers of the two molecular hemispheres.

3.2.3. The furthest center

The radius vectors $\vec{r}(c_1)$ and $\vec{r}(c_2)$, from the origin to c_1 and c_2, respectively, are given by equation (8). Their magnitudes are found (after some algebra) to be

$$\frac{r^2(c_q)}{r_0^2} = 4\left(\ell^2 + k^2 - k\ell\right) + \left\{\frac{h}{2r_0} + (-1)^q\left[\sqrt{3}\ell\cos\phi + (2k-\ell)\sin\phi\right]\tan\theta\right\}^2 - \left(\frac{h\cos\theta}{2r_0}\right)^2, \quad q = 1, 2. \tag{15}$$

To underline the ℓ and k dependence of $r(c_q)$ we rewrite it (again after some algebra) as

$$\frac{r^2(c_q)}{r_0^2} = 4k^2\left(1 + \sin^2\phi\tan^2\theta\right) + \ell^2\left[4 + \left(\sqrt{3}\cos\phi - \sin\phi\right)^2\tan^2\theta\right] + 4k\ell\left[\left(\sqrt{3}\cos\phi - \sin\phi\right)\sin\phi\tan^2\theta - 1\right] + \left(\frac{h\sin\theta}{2r_0}\right)^2 + (-1)^q 2k\frac{h}{r_0}\sin\phi\tan\theta + (-1)^q\ell\frac{h}{r_0}\left(\sqrt{3}\cos\phi - \sin\phi\right)\tan\theta, \quad q = 1, 2, \tag{16}$$

or as

$$r(c_q) = r_0\sqrt{4k^2A_0 + 4k\ell B_1 + 4(-1)^q kB_2 + \ell^2C_1 + 2(-1)^q\ell C_2 + C_3}, \quad q = 1, 2, \tag{17}$$

with

$$A_0 = 1 + \sin^2\phi\tan^2\theta, \tag{18a}$$

$$B_1 = \left(\sqrt{3}\cos\phi - \sin\phi\right)\sin\phi\tan^2\theta - 1, \tag{18b}$$

$$B_2 = \left(\frac{h\sin\theta}{2r_0}\right)\sin\phi\sec\theta, \tag{18c}$$

$$C_1 = 4 + \left(\sqrt{3}\cos\phi - \sin\phi\right)^2\tan^2\theta, \tag{18d}$$

$$C_2 = \left(\frac{h\sin\theta}{2r_0}\right)\left(\sqrt{3}\cos\phi - \sin\phi\right)\sec\theta, \tag{18e}$$

$$C_3 = \left(\frac{h\sin\theta}{2r_0}\right)^2. \tag{18f}$$

Finally, let $R_{\ell k}$ be *the radius of the smallest virtual domain cylinder that fully includes this molecule centered at the lattice site whose radius vector is* $\vec{r}_{\ell k}(\theta, \phi)$*, then*

$$R_{\ell k} = r_{\max} = \max\left\{r(c_1), r(c_2)\right\} + r_0. \tag{19}$$

3.3. The inverse problem

We now have the necessary results to solve the inverse problem: *given a virtual domain cylinder with radius R, determine the range of values of* ℓ *and k subject to the constraint that all molecules centered at lattice sites whose radius vectors are* $\vec{r}_{\ell k}(\theta, \phi)$*, are fully included in the virtual domain cylinder.*

3.3.1. The general constraint

For a molecule to be fully contained in the cylindrical domain, its projection on the half-way plane must be fully contained inside the domain disc (cross-section of the domain cylinder in the half-way plane). This disk has radius R. This inclusion condition is, of course, guaranteed if the furthest point of the molecular projection is less than or equal to R. Hence, the condition that a molecule centered at $\vec{r}_{\ell k}(\theta, \phi)$ be completely contained in the virtual cylindrical domain of radius R is given by the constraint $R_{\ell k} \leqslant R$. This is equivalent to the two simultaneous constraints $r(c_q) \leqslant R - r_0$ for $q = 1, 2$, and, since, on physical grounds, both sides are positive, then the inequality can be more conveniently written as

$$\frac{r^2(c_q)}{r_0^2} - \left(\frac{R - r_0}{r_0}\right)^2 \leqslant 0, \quad q = 1, 2, \tag{20}$$

or simply as

$$f_q(\ell, k) \leqslant 0, \quad q = 1, 2, \tag{21}$$

where, using equation (17), the expression for $f_q(\ell, k)$ is found to be

$$f_q(\ell, k) = 4k^2 A_0 + 4k\ell B_1 + 4(-1)^q k B_2 + \ell^2 C_1 + 2(-1)^q \ell C_2 + C_3 - \left(\frac{R - r_0}{r_0}\right)^2, \quad q = 1, 2. \tag{22}$$

We have suppressed the dependence of the above coefficients on θ and ϕ, in order to simplify the notation and bring out the dependence of $f_q(\ell, k)$ on ℓ and k.

3.3.2. The constraints on k

3.3.2.1. The functions $f_q(\ell, k)$. The function $f_q(\ell, k)$ is a second-order polynomial in k, and can be written as

$$f_q(\ell, k) = 4k^2 A_0 + 4k B_0(\ell, q) + C_0(\ell, q), \tag{23}$$

where A_0 is given by equation (18a), while $B_0(\ell, q)$ and $C_0(\ell, q)$ are defined by

$$B_0(\ell, q) = \ell B_1 + (-1)^q B_2, \qquad q = 1, 2, \tag{24a}$$

$$C_0(\ell, q) = \ell^2 C_1 + 2(-1)^q \ell C_2 + C_3 - \left(\frac{R - r_0}{r_0}\right)^2, \quad q = 1, 2, \tag{24b}$$

with B_1, B_2, C_1, C_2 and C_3 given by equations (18). Explicitly, the coefficients in equation (23) are given by

$$A_0 = 1 + \sin^2\phi \tan^2\theta, \tag{25a}$$

$$B_0(\ell, q) = -\ell + \left[(-1)^q \left(\frac{h}{2r_0}\right) + \ell\left(\sqrt{3}\cos\phi - \sin\phi\right)\tan\theta\right]\sin\phi\tan\theta, \quad q = 1, 2, \tag{25b}$$

$$C_0(\ell,q)=4\ell^2+\left[\left(\frac{h}{2r_0}\right)+(-1)^q\ell\left(\sqrt{3}\cos\phi-\sin\phi\right)\tan\theta\right]^2 - \left[\left(\frac{R-r_0}{r_0}\right)^2+\left(\frac{h\cos\theta}{2r_0}\right)^2\right],\quad q=1,2. \tag{25c}$$

3.3.2.2. The roots of $f_q(\ell,k)$. We will now proceed to evaluate the roots $k_<(\ell,q)$ and $k_>(\ell,q)$ of $f_q(\ell,k)$. Since $A_0\geqslant 0$, then the smaller and larger of the two roots of $f_q(\ell,k)$ are given respectively by

$$k_<(\ell,q)=\frac{-B_0(\ell,q)-\sqrt{\Delta(\ell,q)}}{2A_0},\quad q=1,2, \tag{26a}$$

and

$$k_>(\ell,q)=\frac{-B_0(\ell,q)+\sqrt{\Delta(\ell,q)}}{2A_0},\quad q=1,2, \tag{26b}$$

where $\Delta(\ell,q)$ is given by

$$\Delta(\ell,q)=\left[B_0(\ell,q)\right]^2-A_0C_0(\ell,q),\quad q=1,2, \tag{27}$$

which, when worked out explicitly, gives, after some algebra,

$$\Delta(\ell,q)=-3\ell^2\sec^2\theta-(-1)^q2\sqrt{3}\ell\left(\frac{h}{2r_0}\right)\cos\phi\tan\theta + \left[\left(\frac{R-r_0}{r_0}\right)^2-\left(\frac{h\sin\theta}{2r_0}\right)^2\right]\cos^2\phi+\left(\frac{R-r_0}{r_0}\right)^2\sin^2\phi\sec^2\theta, \tag{28}$$

or alternatively,

$$\Delta(\ell,q)=\left(\frac{R-r_0}{r_0}\right)^2\left[1+\sin^2\phi\tan^2\theta\right]-\left[\left(\frac{h\sin\theta}{2r_0}\right)\cos\phi+(-1)^q\sqrt{3}\ell\sec\theta\right]^2,\quad q=1,2. \tag{29}$$

Combining equations (25) with equations (26) and (29) we obtain the following explicit expressions for the roots of $f_q(\ell,k)$:

$$k_<(\ell,q) = \frac{1}{2[1+\sin^2\phi\tan^2\theta]} \times\left\{\ell-\left[(-1)^q\left(\frac{h}{2r_0}\right)+\ell\left(\sqrt{3}\cos\phi-\sin\phi\right)\tan\theta\right]\sin\phi\tan\theta - \sqrt{\left(\frac{R-r_0}{r_0}\right)^2\left[1+\sin^2\phi\tan^2\theta\right]-\left[\left(\frac{h\sin\theta}{2r_0}\right)\cos\phi+(-1)^q\sqrt{3}\ell\sec\theta\right]^2}\right\},\quad q=1,2, \tag{30a}$$

and

$$k_{>}(\ell, q) = \frac{1}{2[1+\sin^2\phi\tan^2\theta]} \times \left\{ \ell - \left[(-1)^q \left(\frac{h}{2r_0} \right) + \ell\left(\sqrt{3}\cos\phi - \sin\phi\right)\tan\theta \right] \sin\phi\tan\theta + \sqrt{\left(\frac{R-r_0}{r_0} \right)^2 \left[1+\sin^2\phi\tan^2\theta\right] - \left[\left(\frac{h\sin\theta}{2r_0} \right)\cos\phi + (-1)^q\sqrt{3}\ell\sec\theta \right]^2} \right\}, \quad q = 1, 2. \tag{30b}$$

3.3.2.3. The allowed values of k. The allowed values of k are those that guarantee that $f_q(\ell, k)$ is negative for both values of q in accordance with equations (21). Now $f_q(\ell, k)$ is a second-order polynomial in k, and since the coefficient of k^2 in $f_q(\ell, k)$ is positive definite (as can be seen from equations (23) and (25a)), then $f_q(\ell, k)$ is negative, whenever k lies in-between the roots. Thus, due to inequalities (21), the allowed values of k are those that lie simultaneously between the roots of $f_1(\ell, k)$ and the roots of $f_2(\ell, k)$. Since $k_{<}(\ell, q)$ and $k_{>}(\ell, q)$ are respectively the smaller and the larger of the two roots of $f_q(\ell, k)$, then constraints (21) are equivalent to

$$k_{<}(\ell, q) \leqslant k \leqslant k_{>}(\ell, q), \quad q = 1, 2. \tag{31}$$

Since k must be integer, then the allowed range of values of k is further restricted to

$$k_{\min}(\ell, q) \leqslant k \leqslant k_{\max}(\ell, q), \quad q = 1, 2, \tag{32a}$$

where

$$k_{\min}(\ell, q) = \left[k_{<}(\ell, q)\right]^{+} \quad \text{and} \quad k_{\max}(\ell, q) = \left[k_{>}(\ell, q)\right]^{-}, \qquad q = 1, 2. \tag{32b}$$

As defined in [1], $[x]^{+}$ is the smallest integer greater or equal to x (ceiling of x), and $[x]^{-}$ is the largest integer smaller or equal to x (floor of x). Thus, the allowed values of k are those in the interval formed by the intersection of the intervals $[k_{\min}(\ell, 1), k_{\max}(\ell, 2)]$ and $[k_{\min}(\ell, 2), k_{\max}(\ell, 2)]$:

$$\operatorname{Rang} k(\ell) = \left[k_{\min}(\ell, 1), k_{\max}(\ell, 1)\right] \cap \left[k_{\min}(\ell, 2), k_{\max}(\ell, 2)\right]. \tag{33}$$

We define $k_{\min}(\ell)$ and $k_{\max}(\ell)$ respectively as the minimum and maximum values of k in this interval. That is,

$$k_{\min}(\ell) = \min\left\{\operatorname{Rang} k(\ell)\right\}, \tag{34a}$$

$$k_{\max}(\ell) = \max\left\{\operatorname{Rang} k(\ell)\right\}. \tag{34b}$$

So, the constraint that the values of k must satisfy is

$$k_{\min}(\ell) \leqslant k \leqslant k_{\max}(\ell). \tag{35}$$

3.3.3. The constraints on ℓ

3.3.3.1. The functions $\Delta(\ell, q)$. Equation (29) for $\Delta(\ell, q)$ can be written as

$$\Delta(\ell, q) = \alpha\ell^2 + 2\beta_q\ell + \gamma, \quad q = 1, 2, \tag{36}$$

with

$$\alpha = -3\sec^2\theta, \tag{37a}$$

$$\beta_q = (-1)^{q+1}\sqrt{3}\left(\frac{h}{2r_0}\right)\cos\phi\tan\theta, \quad q = 1, 2, \tag{37b}$$

$$\gamma = \left[\left(\frac{R - r_0}{r_0}\right)^2 - \left(\frac{h\sin\theta}{2r_0}\right)^2\right]\cos^2\phi + \left(\frac{R - r_0}{r_0}\right)^2\sin^2\phi\sec^2\theta. \tag{37c}$$

We note that $\alpha \leqslant 0$, and, due to constraint (5), $\gamma \geqslant 0$. On the other hand, β_q can be positive or negative, depending on the value of q.

3.3.3.2. The roots of $\Delta(\ell, q)$. Since the coefficient of ℓ^2 in $\Delta(\ell, q)$ is negative, then the ordering of the roots of $\Delta(\ell, q)$ is

$$\ell_<(q) = \frac{-\beta_q + \sqrt{\beta_q^2 - \alpha\gamma}}{\alpha}, \quad q = 1, 2, \tag{38a}$$

and

$$\ell_>(q) = \frac{-\beta_q - \sqrt{\beta_q^2 - \alpha\gamma}}{\alpha}, \quad q = 1, 2. \tag{38b}$$

Making use of equations (37), and restricting the range of θ to $0 \leqslant \theta \leqslant \pi/2$, the explicit expressions for the above roots take the form

$$\ell_<(q) = \frac{1}{\sqrt{3}}\left\{-\sqrt{\left(\frac{R - r_0}{r_0}\right)^2\left(\cos^2\theta\cos^2\phi + \sin^2\phi\right)}\right.$$
$$\left. + (-1)^{q+1}\left(\frac{h\sin\theta}{2r_0}\right)\cos\theta\cos\phi\right\}, \qquad 0 \leqslant \theta \leqslant \frac{\pi}{2}, \quad q = 1, 2, \tag{39a}$$

and

$$\ell_>(q) = \frac{1}{\sqrt{3}}\left\{\sqrt{\left(\frac{R - r_0}{r_0}\right)^2\left(\cos^2\theta\cos^2\phi + \sin^2\phi\right)}\right.$$
$$\left. + (-1)^{q+1}\left(\frac{h\sin\theta}{2r_0}\right)\cos\theta\cos\phi\right\}, \qquad 0 \leqslant \theta \leqslant \frac{\pi}{2}, \quad q = 1, 2. \tag{39b}$$

The product of the roots of $\Delta(\ell, q)$ is given by

$$\ell_<(q)\ell_>(q) = \frac{\gamma}{\alpha} \leqslant 0, \quad q = 1, 2. \tag{40a}$$

That the product of the roots is non-positive, follows from the fact that α is non-positive, and γ is non-negative. Equation (40a) guarantees that the larger root is non-negative and the smaller root is non-positive:

$$\ell_<(q) \leqslant 0 \quad \text{and} \quad \ell_>(q) \geqslant 0, \qquad q = 1, 2. \tag{40b}$$

3.3.3.3. The allowed values of ℓ. The allowed values of ℓ are those for which $k_<(\ell, q)$ and $k_>(\ell, q)$ are both real. This will be true provided that $\Delta(\ell, q)$ is positive. Since $\Delta(\ell, q)$ is a second-order polynomial in ℓ, and since the coefficient of ℓ^2 is negative (as can be seen from equation (37a)), then $\Delta(\ell, q)$ is positive for values of ℓ in-between the roots of $\Delta(\ell, q)$:

$$\ell_<(q) \leqslant \ell \leqslant \ell_>(q), \quad q = 1, 2. \tag{41}$$

Since ℓ must be integer, then inequality (41) should be further restricted to

$$\ell_{\min}(q) \leqslant \ell \leqslant \ell_{\max}(q), \quad q = 1, 2, \tag{42a}$$

where

$$\ell_{\min}(q) = \big[\ell_<(q)\big]^+ \quad \text{and} \quad \ell_{\max}(q) = \big[\ell_>(q)\big]^-, \qquad q = 1, 2. \tag{42b}$$

If we define $\ell_{\min}$ and $\ell_{\max}$ by

$$\ell_{\min} = \max\big\{\ell_{\min}(1), \ell_{\min}(2)\big\} \quad \text{and} \quad \ell_{\max} = \min\big\{\ell_{\max}(1), \ell_{\max}(2)\big\}, \tag{43a}$$

then the two simultaneous inequalities (42a) can be combined into

$$\ell_{\min} \leqslant \ell \leqslant \ell_{\max}. \tag{43b}$$

Since $\sin\theta \geqslant 0$, in the range $0 \leqslant \theta \leqslant \pi/2$, then it is easy to see, from equations (39a) for $\ell_<(q)$ and (39b) for $\ell_>(q)$, that the following relations hold:

$$\ell_{\min} = \left[-\frac{1}{\sqrt{3}}\left\{\sqrt{\left(\frac{R - r_0}{r_0}\right)^2\left(\cos^2\theta\cos^2\phi + \sin^2\phi\right)} + \left(\frac{h\sin\theta}{2r_0}\right)|\cos\phi|\cos\theta\right\}\right]^+, \quad 0 \leqslant \theta \leqslant \frac{\pi}{2}, \tag{44a}$$

and

$$\ell_{\max} = \left[\frac{1}{\sqrt{3}}\left\{\sqrt{\left(\frac{R - r_0}{r_0}\right)^2\left(\cos^2\theta\cos^2\phi + \sin^2\phi\right)} - \left(\frac{h\sin\theta}{2r_0}\right)|\cos\phi|\cos\theta\right\}\right]^-, \quad 0 \leqslant \theta \leqslant \frac{\pi}{2}. \tag{44b}$$

Using the identity $[-x]^+ = -[x]^-$, we have

$$\ell_{\min} = -\ell_{\max}. \tag{45}$$

The range of values of ℓ as given by (43b) does guarantee that $k_{\min}(\ell, q)$ and $k_{\max}(\ell, q)$ are real for both $q = 1$ and $q = 2$. On the other hand, it does not guarantee that the range of allowed values of k, $\mathrm{Rang}\, k(\ell)$, as given by equation (33), is not empty. Hence, the range of values of ℓ may be smaller than that given by (43b), and corresponds to values of ℓ within this range for which $\mathrm{Rang}\, k(\ell) \neq \emptyset$ ($\emptyset$ being the empty set). Hence, equation (43b) should be replaced by

$$\overline{\ell}_{\min} \leqslant \ell \leqslant \overline{\ell}_{\max}, \tag{46}$$

where

$$\overline{\ell}_{\min} = \min\left\{\ell \mid \ell_{\min} \leqslant \ell \leqslant \ell_{\max};\, \mathrm{Rang}\, k\left(\overline{\ell}_{\min}\right) \neq \emptyset\right\} \tag{47a}$$

and

$$\overline{\ell}_{\max} = \max\left\{\ell \mid \ell_{\min} \leqslant \ell \leqslant \ell_{\max};\, \mathrm{Rang}\, k\left(\overline{\ell}_{\max}\right) \neq \emptyset\right\}. \tag{47b}$$

3.4. The boundary

The radius of the virtual domain is the smallest virtual cylinder radius that fully contains the physical domain. By combining the solutions of the direct and inverse problems solved above, we can determine the radius of the virtual domain. This is done in two iterations. First given a radius R, we determine the values of $k_{\min}(\ell)$ and $k_{\max}(\ell)$ via equation (34), and the values of $\overline{\ell}_{\min}$ and $\overline{\ell}_{\max}$ via equation (47). Then the minimal domain radius is given by

$$R_{\min} = \max\left[R_{k\ell} \mid k_{\min}(\ell) \leqslant k \leqslant k_{\max}(\ell);\ \overline{\ell}_{\min} \leqslant \ell \leqslant \overline{\ell}_{\max}\right], \tag{48}$$

where $R_{k\ell}$ is the radius of the circle circumscribing the projection on the half-way plane of the molecule centered at the lattice site corresponding to (ℓ, k). It is given by equation (19). The rigorous analytic solution of the above optimization problem (48) opens up a whole new chapter of investigation and will not be dealt with here. Since all expressions appearing on the right-hand side of (48) are analytic, the numerical solution of the above equation is easily handled by any computer. This, of course, is one of the major reasons for pushing the analytic solution as far as possible.

4. The number of molecules and packing fraction

4.1. The number of molecules

The number of molecules in a domain is the number of occupied lattice sites. There is one lattice site for every allowed pair of values (ℓ, k). The allowed values of ℓ are given via equations (47), and for every allowed value of ℓ the number N_ℓ of allowed values of k is given by

$$N_\ell = k_{\max}(\ell) - k_{\min}(\ell) + 1, \tag{49}$$

where $k_{\min}(\ell)$, $k_{\max}(\ell)$ are given by equation (34).

The number N of spheromolecules of radius r_0, of cylindrical length h, of inclination θ in the direction ϕ, in a domain of radius $\leqslant R$ is obtained by summing N_ℓ over all allowed values of ℓ:

$$N = \sum_{\ell=\overline{\ell}_{\min}}^{\overline{\ell}_{\max}} N_\ell = \sum_{\ell=\overline{\ell}_{\min}}^{\overline{\ell}_{\max}} \left[k_{\max}(\ell) - k_{\min}(\ell) + 1\right], \tag{50}$$

where $\overline{\ell}_{\min}$ and $\overline{\ell}_{\max}$ are given by equation (47).

4.2. Packing fraction

Once N is evaluated, the packing fraction can be calculated. Since the problem of arbitrarily inclined molecules is inherently three-dimensional, we will define the packing fraction β as the ratio of the volume occupied by the molecules to the total volume of the virtual domain cylinder:

$$\beta = N\frac{V_{\mathrm{m}}}{V_{\mathrm{D}}}, \tag{52}$$

where V_{m} and V_{D} are the volume of a spheromolecule and the volume of the cylindrical domain, respectively. They are given by

$$V_{\mathrm{m}} = \pi r_0^2\left(h + \frac{4}{3}r_0\right), \tag{53a}$$

$$V_{\mathrm{D}} = \pi\left(h\cos\theta + 2r_0\right)R_{\min}^2. \tag{53b}$$

Hence,

$$\beta = \frac{(1 + 4r_0/3h)(r_0/R_{\min})^2}{(\cos\theta + 2r_0/h)}N, \tag{54}$$

where $R_{\min}$ and N are given by equations (48) and (50), respectively.

5. Results and discussion

5.1. Input and output parameters

The analytic results obtained here permit us to make an extensive study of the static structure of domains made up of arbitrarily oriented spherocylindrical molecules aligned parallel to each other, in terms of the four inherent dimensionless input parameters of the problem. These input parameters are:

(i) R/r_0, the upper bound on the domain radius in units of the molecular radius r_0;

(ii) h/r_0, the length of the cylindrical part of the molecule in units of r_0;

(iii) θ, the angle of inclination of the molecular axes with respect to the normal to the interface;

(iv) ϕ, the direction of inclination of the molecular axes.

The output parameters are:

(i) $\{(\ell, k)\}$, the set of occupied lattice sites;

(ii) $R_{\min}$, the radius of the domain;

(iii) N, the number of molecules in the domain;

(iv) β, the packing fraction.

An extensive numerical study of the static domain structure in terms of the four independent input parameters is too voluminous to include in the present article. Furthermore, the main usefulness of analytic results, like the ones obtained here, is to render such numerical studies superfluous. Hence, we will instead restrict the discussion to a systematic understanding of the structure of the solution.

5.2. *The length scale*

The first scale of the problem is determined by the atomic parameters r_{H} and r_{C}, the single-bonded covalent radii of the hydrogen and carbon atoms, respectively [16]. The second scale is set by the molecular radius r_0 (the radius of the cylindrical part of the molecule), and the relative length h/r_0 of the cylindrical part of the molecule. These molecular parameters are given [2, equation (36)] in terms of the atomic radii r_{H} and r_{C}, the tetrahedral angle χ, and the number n of carbon atoms in the aliphatic chain [16–18]. For organic molecules of biological interest in Langmuir films [19–22], the value of the molecular radius is $r_0 = 1.36$ Å, while the value of h/r_0 ranges from 16 to 22 as shown in [2, table 1]. We take the value $h/r_0 = 20$ as a "standard" value. The results obtained in the present work are all scale invariant under a change in the value of r_0. The third scale is determined by the domain radius, R/r_0, which is a function of the number N, dimension h/r_0 and orientation (θ, ϕ) of the molecules in the domain. The fourth scale determines the film structure in terms of the domain parameters, and will be dealt with subsequently.

5.3. *Graphic simulation*

All the figures appearing in this article are high resolution graphics [23] programmed using the equations developed in this work. They are three-dimensional virtual reality rendering of the packing of spherocylindrical molecules inside a right circular cylindrical domain. Their visual appearance provides confirmation of the validity of the algebraic results obtained here. Quantitatively, the number of molecules in a domain can be counted off the graphs and compared with the number predicted by equation (50). We can perform such "graphic experiments" at will, and in all cases the visual and algebraic results agree.

As an example consider figure 2, depicting the packing of spherocylindrical molecules inside a right circular cylindrical domain, for "standard" molecules ($h/r_0 = 20$), inclined at an angle $\theta = 30^\circ$ to the normal (to the interface), in a direction $\phi = -45^\circ$, inside a cylindrical domain of relative radius bounded by $R/r_0 = 15$ (leading to

Table 1
Range of k versus ℓ for the allowed values of ℓ. The input parameters are $R/r_0 = 15$, $h/r_0 = 20$, $\theta = 70°$, and $\phi = 45°$. The resulting domain radius is $R_{\min}/r_0 = 14.6055$; the number of molecules is $N = 13$, and the packing fraction is $\beta = 0.147061$.

ℓ	$k_{\min}(\ell, 2)$	$k_{\max}(\ell, 2)$	$k_{\min}(\ell, 1)$	$k_{\max}(\ell, 1)$	Rang $k(\ell)$
4	−4	−2	−1	4	{ }
3	−4	−1	−1	4	{−1}
2	−5	0	−1	4	{−1, 0}
1	−5	0	−1	5	{−1, 0}
0	−5	1	−1	5	{−1, 0, 1}
−1	−5	1	0	5	{0, 1}
−2	−4	1	0	5	{0, 1}
−3	−4	1	1	4	{1}
−4	−4	1	2	4	{ }

$R_{\min}/r_0 = 14.9796$). Furthermore, it is visually apparent that the domain includes the largest number of molecules possible. We count 83 molecules in the domain, and this is the exact result obtained from equation (50). In all figures appearing in this paper, the number of molecules indicated is that calculated according to equation (50). This number can, in each case, be checked visually by counting molecules.

5.4. *The existence of a solution*

The necessary and sufficient condition for a solution to exist (to have a non-empty domain) is that inequality (5) be satisfied. This inequality guarantees that the domain is large enough to accommodate at least one molecule. Technically, each occupied lattice site in the half-way plane is the center of a molecule, and the occupied lattice sites are determined by the allowed values of (ℓ, k). Inequality (5) guarantees, according to equation (40b), that $\ell_<(q) \leqslant 0$ and $\ell_>(q) \geqslant 0$. This in turn, according to equation (42), guarantees that $\ell_{\min}(q) \leqslant 0$ and $\ell_{\max}(q) \geqslant 0$. Consequently, according to equation (43), the set of allowed values of ℓ is not empty, $\ell = 0$ being necessarily a solution. In appendix, we will prove that, for $\ell = 0$, the set of allowed values of k is not empty either, $k = 0$ being necessarily a solution. Hence, when constraint (5) is satisfied, then there is at least one molecule in the domain. It corresponds to $(\ell = 0, k = 0)$, and hence, its center is situated at the center of the cylindrical domain (see equation (3)) which is also the origin of coordinates.

5.5. *The range of k*

Table 1 shows the values of $k_{\min}(\ell, q)$ and $k_{\max}(\ell, q)$ for $q = 1, 2$, as well as Rang $k(\ell)$, for $\ell_{\min} \leqslant \ell \leqslant \ell_{\max}$. According to equation (33), the values of k appearing in Rang $k(\ell)$ are those which simultaneously satisfy the two constraints $k_{\min}(\ell, 1) \leqslant k \leqslant k_{\max}(\ell, 1)$ and $k_{\min}(\ell, 2) \leqslant k \leqslant k_{\max}(\ell, 2)$. When ℓ takes its limiting values $\ell_{\min} = -4$ and $\ell_{\max} = +4$, Rang $k(\ell)$, as seen from table 1, is empty. So, even

Table 2
Output domain parameters versus direction of inclination ϕ. The other input parameters are $R/r_0 = 15$, $h/r_0 = 20$, $\theta = 30°$.

ϕ	$\ell_{\min}$	$\ell_{\max}$	N	$R_{\min}$	β
+90°	−8	8	85	14.8227	0.427171
+80°	−7	7	85	14.8219	0.427221
+70°	−7	7	87	14.9682	0.428766
+60°	−6	6	85	14.6015	0.440216
+50°	−6	6	87	14.9682	0.428766
+40°	−5	5	85	14.8219	0.427221
+30°	−5	5	85	14.8227	0.427171
+20°	−4	4	85	14.8219	0.427221
+10°	−4	4	87	14.9682	0.428766
0°	−4	4	85	14.6015	0.440216
−10°	−4	4	87	14.9682	0.428766
−20°	−4	4	85	14.8219	0.427221
−30°	−5	5	85	14.8227	0.427171
−40°	−5	5	85	14.8219	0.427221
−50°	−6	6	87	14.9682	0.428766
−60°	−6	6	85	14.6015	0.440216
−70°	−7	7	87	14.9682	0.428766
−80°	−7	7	85	14.8219	0.427221
−90°	−8	8	85	14.8227	0.427171

though the constraints on ℓ allow it to take all values in the interval $\ell_{\min} \leqslant \ell \leqslant \ell_{\max}$ with $\ell_{\min} = -4$ and $\ell_{\max} = +4$, only values of ℓ in the range $\overline{\ell}_{\min} \leqslant \ell \leqslant \overline{\ell}_{\max}$ with $\overline{\ell}_{\min} = -3$ and $\overline{\ell}_{\max} = +3$ do lead to occupied lattice sites.

The results obtained in table 1 correspond to $R/r_0 = 15$ (imposed upper bound on the domain radius), $h/r_0 = 20$ (length of the cylindrical part of the molecule), $\theta = 70°$ (angle of inclination) and $\phi = 45°$ (direction of inclination), leading to $\ell_{\min} = -4$, $\ell_{\max} = +4$, $R_{\min}/r_0 = 14.6055$ (domain radius), $N = 13$ (number of molecules), and $\beta = 0.147061$ (packing fraction). The number of molecules N can be obtained from table 1, by counting the number of allowed values of k, that is, by summing the lengths of Rang $k(\ell)$ over ℓ from $\ell_{\min} = -4$ to $\ell_{\max} = +4$, or equivalently from $\overline{\ell}_{\min} = -3$ to $\overline{\ell}_{\max} = +3$.

5.6. *The range of ℓ*

Table 2 shows the values of $\ell_{\min}$ and $\ell_{\max}$ as well as N, $R_{\min}/r_0$ and β corresponding to $R/r_0 = 15$, $h/r_0 = 20$, and $\theta = \pi/6$, for values of the angle ϕ scanning the range $-90° \leqslant \phi \leqslant +90°$ by increments of 10°. There are a number of features in table 2 that are worth underlining:

(i) The values of $R_{\min}$, N, and β are symmetric under a rotation of $\phi = \pi/3$ about the z-axis. This is an expected direct consequence of the hexagonal symmetry of the reference lattice as pointed out in section 2.7.2.

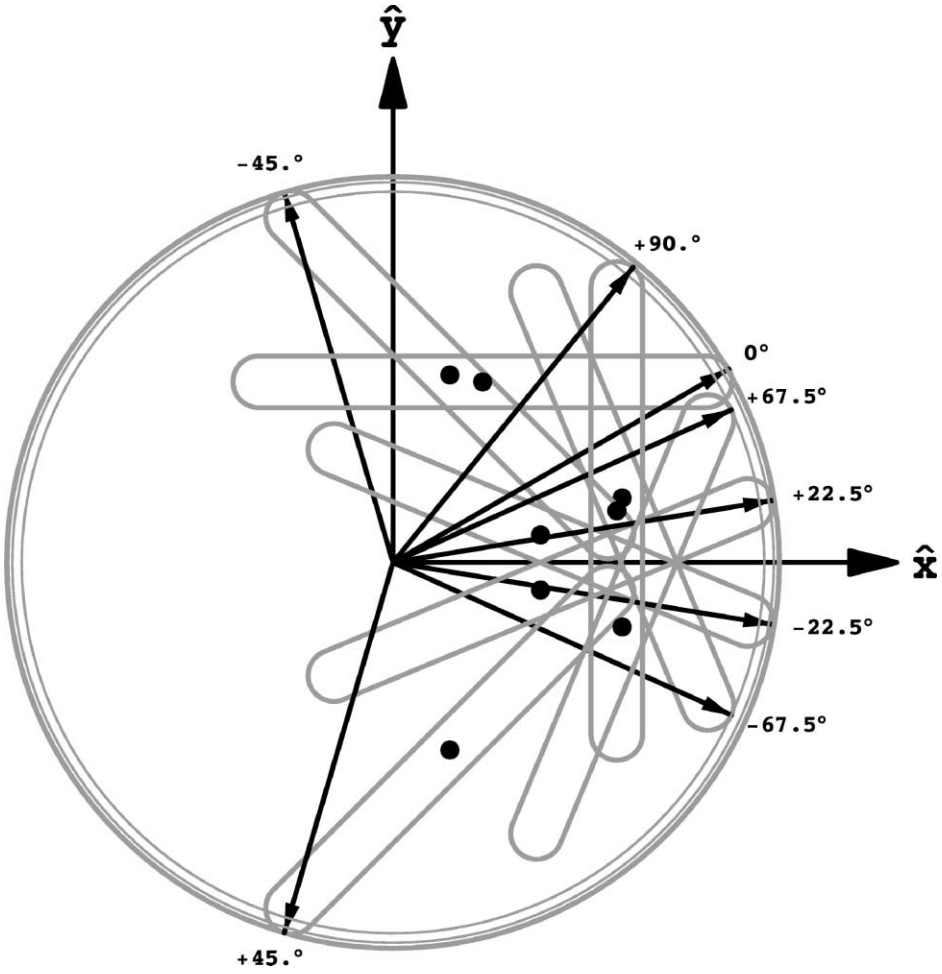

Figure 10. The projection on the half-way plane of the furthest molecule, as a function of the direction of inclination ϕ. Also shown is the vector from the origin to the furthest point as well as the centers of the molecular projections. The parameters used in generating the figure are $r_0 = 1$, $R = 15$, $h = 20$, $\theta = \pi/3$, while ϕ scans the range $-\pi/2 \leqslant \phi \leqslant \pi/2$ by increments of $\pi/8$.

(ii) The largest number of molecules that can be fitted in a cylindrical domain having a radius $\leqslant R$ does not necessarily correspond to the highest density. At $\phi = 10^\circ$ for example, we can accommodate a maximum of 87 molecules. These 87 molecules are fully contained within a cylinder of relative radius $R_{\min}/r_0 = 14.9682$ leading to a packing fraction of $\beta = 0.428766$. On the other hand, if the inclination direction is $\phi = 0^\circ$, then the maximum number of molecules that can be accommodated is only 85. But these molecules are fully contained within a cylinder of relative radius $R_{\min}/r_0 = 14.6015$ leading to a higher packing fraction of $\beta = 0.440216$. So the precise evaluation of $R_{\min}/r_0$, rather than the use of the input upper bound R/r_0, is important.

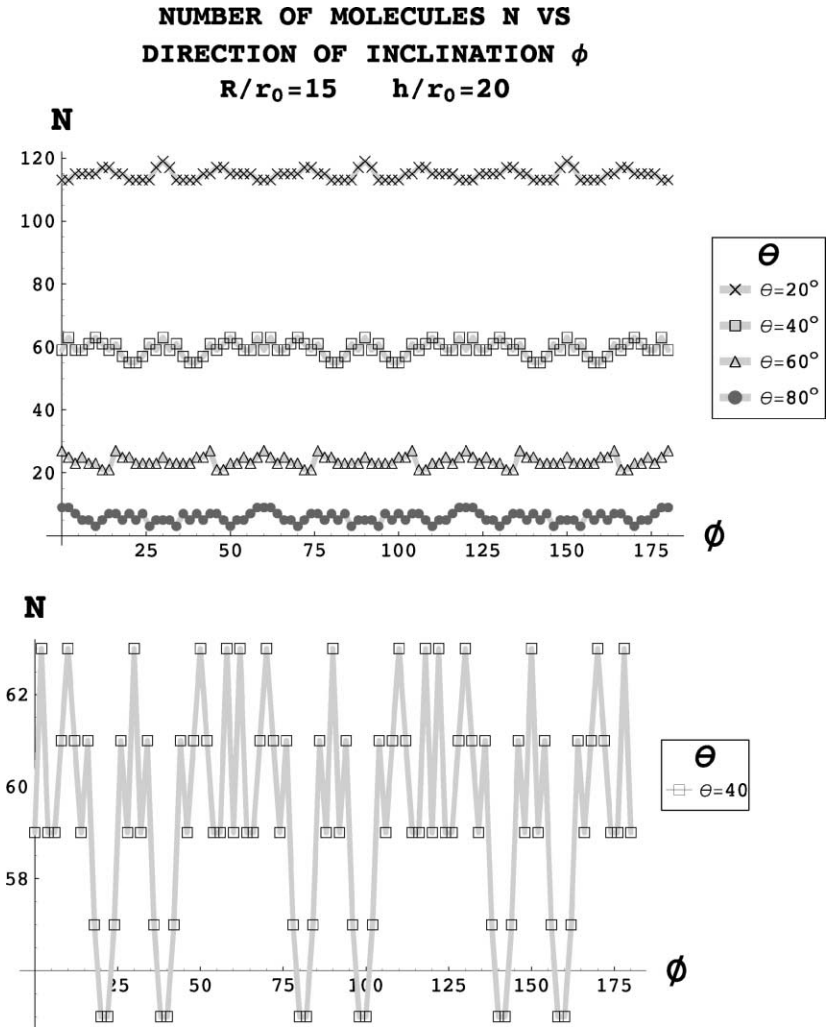

Figure 11. The number N of molecules in a domain as a function of the direction of inclination ϕ, for various values of the inclination angle θ. The values of the other input parameters are $R/r_0 = 15$ and $h/r_0 = 20$. The variation of N with ϕ for the case $\theta = 40^\circ$ is shown amplified in the lower part of the graph.

(iii) Table 2 seems to indicate that the most dense packing corresponds to inclinations in the direction of next nearest neighbors ($\phi = -\pi/3,\ 0,\ +\pi/3$). This is a misleading artifact arising from the specific choice of parameters. The optimal value of ϕ is actually a complicated function of the input parameters R/r_0, h/r_0, and θ.

5.7. The number of molecules

Figure 11 gives the number of molecules N as a function of the direction of inclination ϕ, for different values of the angle of inclination θ. The value of the other input

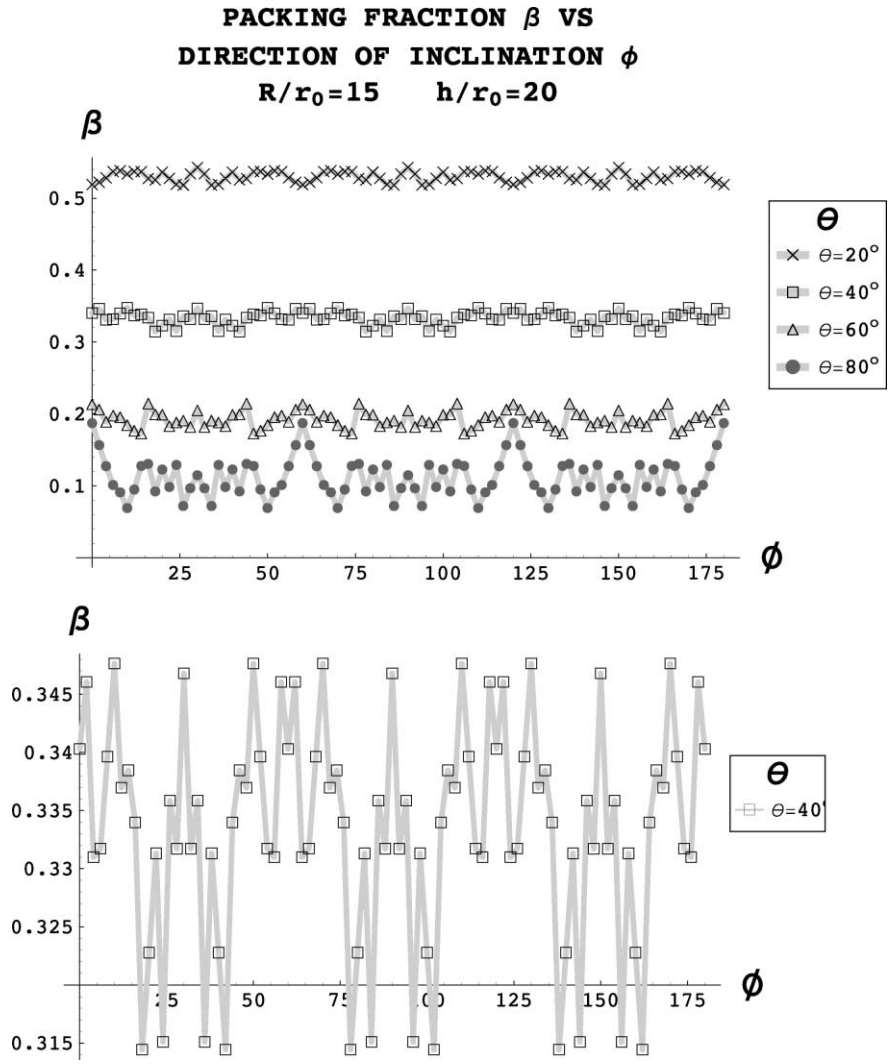

Figure 12. The packing fraction β as a function of the direction of inclination ϕ, for various values of the inclination angle θ. The values of the other input parameters are $R/r_0 = 15$ and $h/r_0 = 20$. The variation of β with ϕ for the case $\theta = 40^\circ$ is shown amplified in the lower part of the graph.

parameters are $R/r_0 = 15$ and $h/r_0 = 20$. It is easily seen that the dependence of the number of molecules on ϕ, is small compared to its dependence on θ. It is also worth noting that the maxima and minima of N as a function of ϕ, vary with θ. The ϕ "signal" corresponding to $\theta = 40^\circ$ is shown amplified in the lower part of the graph.

5.8. The packing fraction

Figure 12 gives the packing fraction β as a function of the direction of inclination ϕ, for different values of the angle of inclination θ. The values of the other input parameters

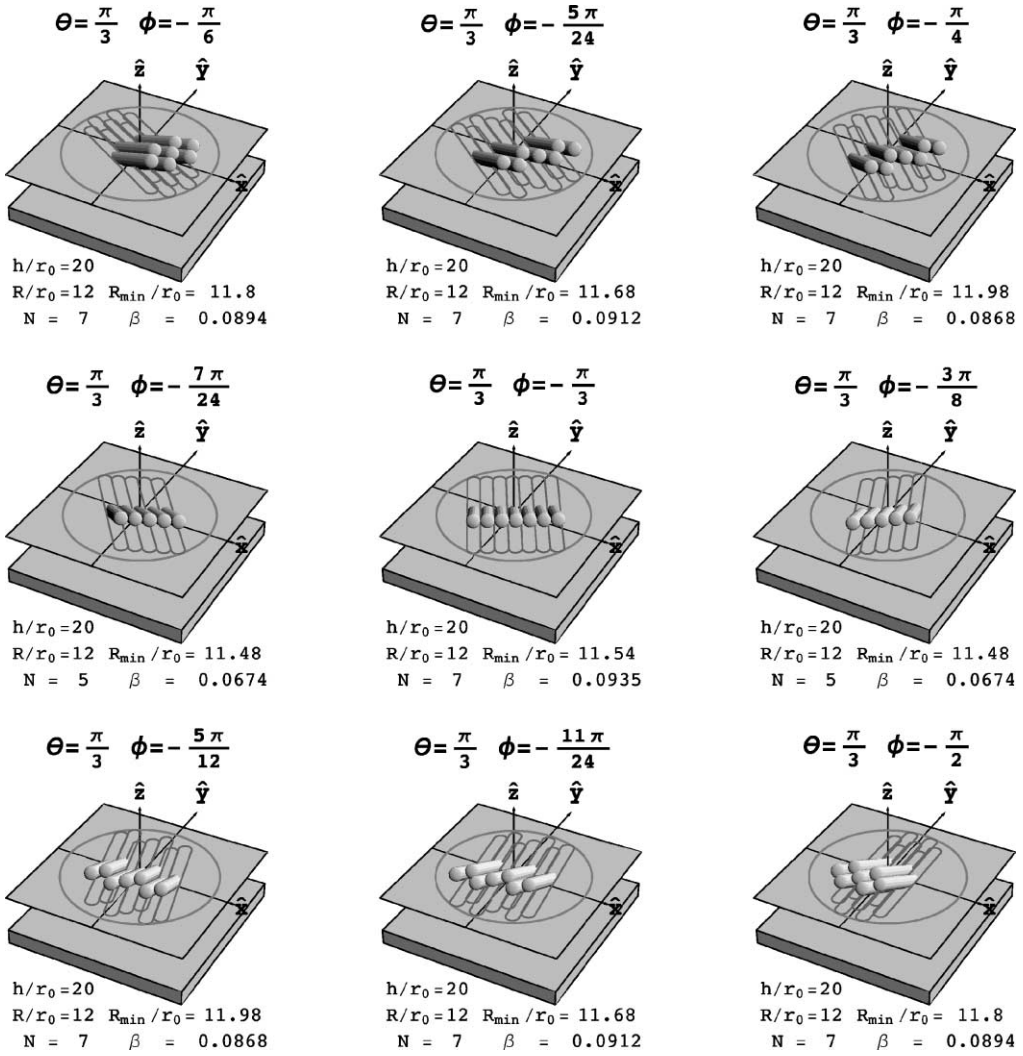

Figure 13. Three-dimensional graphic simulation of the configuration of the domain molecules as a function of the direction of inclination ϕ in the range $-\pi/2 \leqslant \phi \leqslant -\pi/6$. ϕ varies by steps of $\pi/6$. The angle of inclination θ is held fixed at $\theta = \pi/3$, and the other input parameters are $R/r_0 = 12$ and $h/r_0 = 20$.

are $R/r_0 = 15$ and $h/r_0 = 20$. Again, and as expected, the dependence of the packing fraction on ϕ, is small compared to its dependence on θ, and the maxima and minima of β as a function of ϕ, vary with θ. The ϕ "signal" corresponding to $\theta = 40^\circ$ is shown amplified in the lower part of the graph.

5.9. The direction of inclination

Figure 13 shows a three-dimensional graphic simulation of the domain molecules as a function of the direction of inclination ϕ in the range $-\pi/2 \leqslant \phi \leqslant -\pi/6$ by

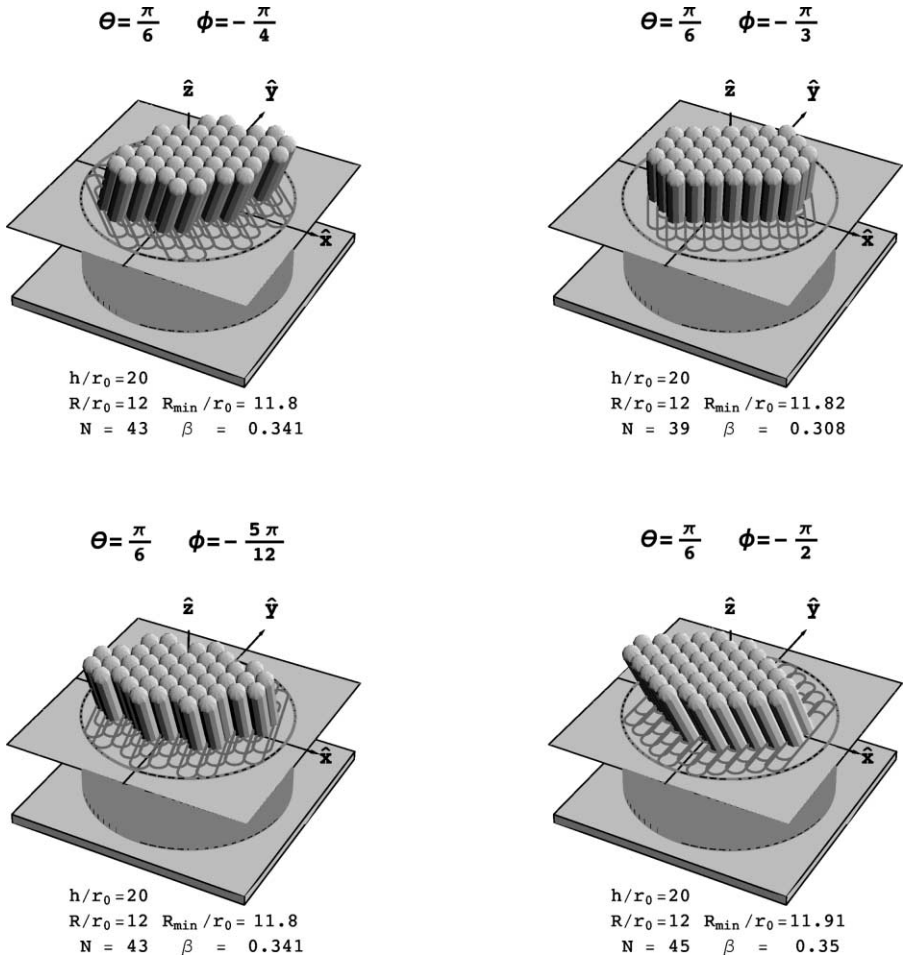

Figure 14. Three-dimensional graphic simulation of the configuration of the domain molecules as a function of the direction of inclination ϕ in the range $-\pi/2 \leqslant \phi \leqslant -\pi/4$. ϕ varies by steps of $\pi/12$. The angle of inclination θ is held fixed at $\theta = \pi/6$, and the other input parameters are $R/r_0 = 12$ and $h/r_0 = 20$.

increments of $\pi/6$. The angle of inclination θ is held fixed at $\theta = \pi/3$, and the other input parameter are $R/r_0 = 12$ and $h/r_0 = 20$. It is easily seen from the figure that the effect of ϕ on the molecular configuration is considerable. The optimal direction of inclination in this case is in the direction of the principal axis of symmetry of the reference lattice, that is, in the direction of the $\hat{y}$-axis (or $\phi = -\pi/2$). Due to the hexagonal symmetry an equivalent optimal configuration must appear $\Delta\phi = \pi/3$ further on, that is, for $\phi = -\pi/6$, and this is actually the case (as is evident from figure 13). The number of molecules varies from 5 to 7, that is, by about 40%. The packing fraction varies between 0.0674 and 0.0935, that is, by about 50%.

Note that the most condensed configurations, those corresponding to $\phi = -\pi/2$ and $\phi = -\pi/6$, do not correspond to the largest packing fraction. Actually the largest

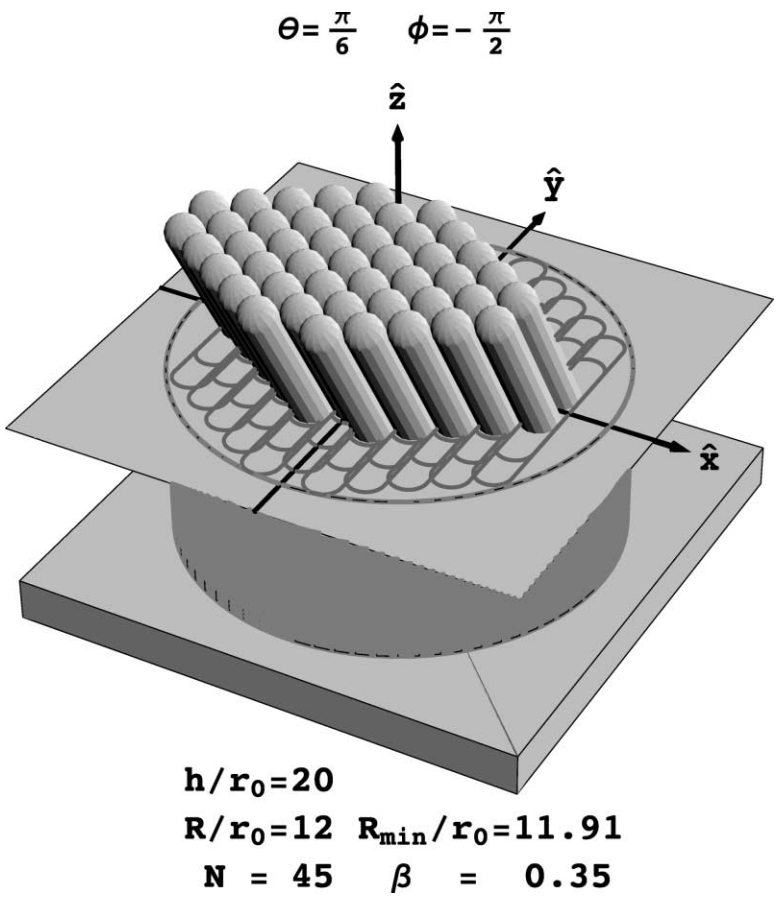

Figure 15. Three-dimensional graphic simulation of the configuration of the domain molecules for $\phi = -\pi/2$ (inclination in the direction of a principal axis of symmetry). The values of the other input parameters are $\theta = \pi/6$, $R/r_0 = 12$ and $h/r_0 = 20$.

packing fraction corresponds to $\phi = -\pi/3$, and for this direction of inclination the molecules are the least compacted. This underlines the fact that the three-dimensional packing fraction as defined by equation (52) is above all a measure useful in inter-domain interactions. The compactness of the molecular configuration (which lowers the Van der Waals domain energy) requires a different (two-dimensional) indicator defined in the cross-sectional plane of the physical domain. The discrepancy between the two indicators increases with increasing molecular inclination and decreasing domain radius. On the other hand, for larger domains or small tilting angles, the two indicators converge.

Figure 14 shows a three-dimensional graphic simulation of the domain molecules as a function of the direction of inclination ϕ in the range $-\pi/2 \leqslant \phi \leqslant -\pi/4$ by increments of $\pi/12$. The angle of inclination θ is held fixed at $\theta = \pi/6$, and the other input parameters are $R/r_0 = 12$ and $h/r_0 = 20$. In spite of the reduced angle of inclination, the effect of ϕ on the molecular configuration is still considerable.

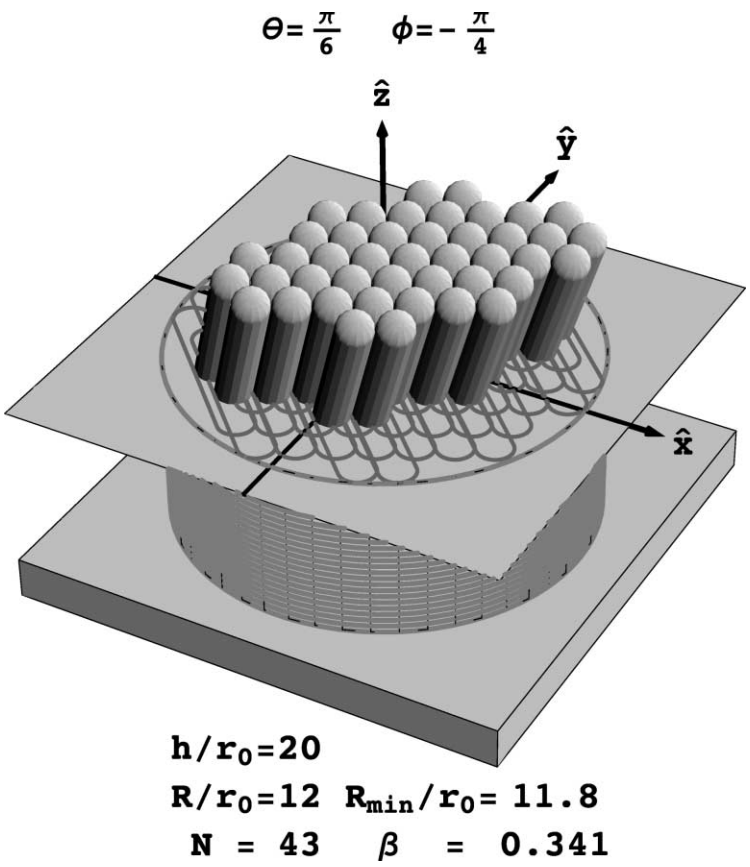

Figure 16. Three-dimensional graphic simulation of the configuration of the domain molecules for $\phi = -\pi/4$. The values of the other input parameters are $\theta = \pi/6$, $R/r_0 = 12$ and $h/r_0 = 20$.

The optimal direction of inclination in this case is again in the direction of the principal axis of symmetry of the reference lattice, that is, in the direction of the $\hat{y}$-axis (or $\phi = -\pi/2$). But now maximum compactness is in phase with the maximum value of the three-dimensional packing fraction. The value of N varies between 39 and 45, the value of β varies between 0.308 and 0.350 (about 15% variation in both cases).

Figures 15–17 show an enlargement of the domain for three characteristic directions: (i) $\phi = -\pi/2$ (inclination in the direction of a principal axis of symmetry), (ii) $\phi = 0$ (inclination in the direction of a secondary axis of symmetry), and (iii) inclination in the intermediate direction $\phi = -\pi/4$. In all three cases, the input parameters are $\theta = \pi/6$, $R/r_0 = 12$ and $h/r_0 = 20$.

6. Conclusion

This paper presents a theoretical model for the organization of phospholipidic molecular domains in Langmuir films at the gas/liquid interface. The molecules of the

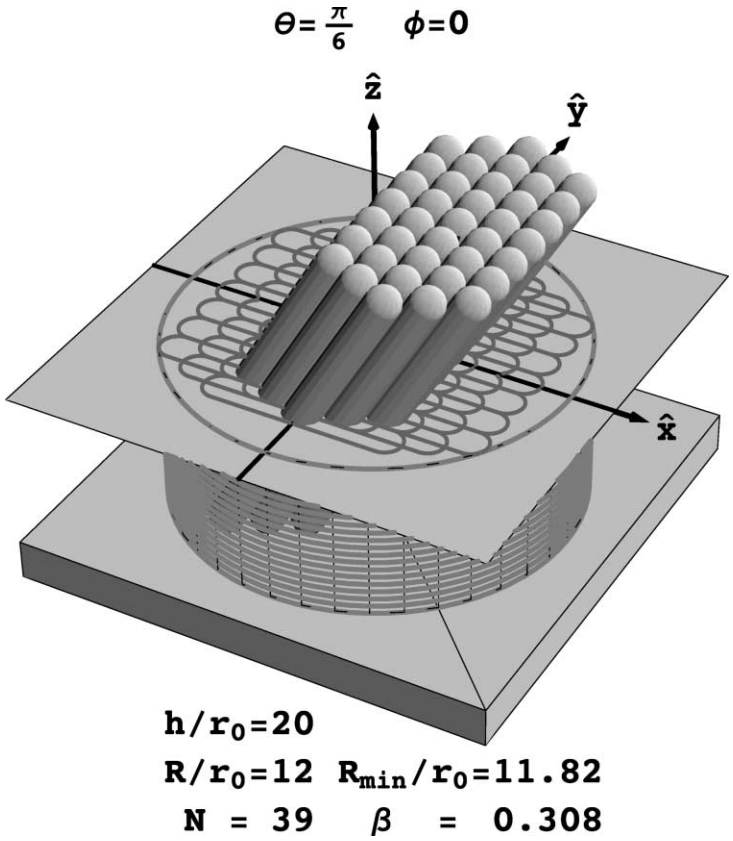

Figure 17. Three-dimensional graphic simulation of the configuration of the domain molecules for $\phi = 0$ (inclination in the direction of a secondary axis of symmetry). The values of the other input parameters are $\theta = \pi/6$, $R/r_0 = 12$ and $h/r_0 = 20$.

domain are modeled as spherocylinders. They are rigid, close packed, and aligned parallel to each other. Their collective orientation is completely arbitrary. The molecular organization is described by four input parameters. These are h/r_0, R/r_0, θ and ϕ. The molecular radius r_0 (which sets the scale), and the length h of the cylindrical part of the molecule, are given in terms of atomic parameters. R is the input domain radius, and (θ, ϕ) are the spherical angles that determine the orientation of the molecular axes.

In terms of these input parameters, we determine the molecular organization of the domain. Specifically, analytic expressions are obtained for $\ell_{\min}$, $\ell_{\max}$, $k_{\min}(\ell)$ and $k_{\max}(\ell)$. These parameters define the boundaries of the set of allowed values of (ℓ, k). These latter, in turn, determine, via equation (3), the positions of the centers of the molecules of the domain. In the language of this article, they determine the occupied lattice sites in the half-way plane. We thus obtain an analytic determination of the static structural organization of the domain including boundaries.

As a first application, we evaluate the domain radius $R_{\min}$, the number N of molecules in the domain, and the packing fraction β. $R_{\min}$ varies almost linearly with R, but

does not vary significantly with θ and ϕ. As for N, the hierarchy of influence of the input parameters is R, θ, ϕ. For β, on the other hand, this hierarchy is more complicated and itself varies with the value of R. Finally, the dependence of the molecular configuration on the direction of inclination ϕ is considerable, and more than what was expected intuitively.

Appendix

In this appendix, we want to prove that, for $\ell = 0$, the set of allowed values of k is not empty, $k = 0$ being necessarily a solution. To prove this we note that for $\ell = 0$, equations (30) reduce to

$$k_<(0,q) = -\frac{1}{2[1+\sin^2\phi\tan^2\theta]} \times\left\{(-1)^q\left(\frac{h}{2r_0}\right)\sin\phi\tan\theta + \sqrt{\left(\frac{R-r_0}{r_0}\right)^2\left[1+\sin^2\phi\tan^2\theta\right]-\left(\frac{h\sin\theta}{2r_0}\right)^2\cos^2\phi}\right\}, \quad q=1,2, \tag{A.1a}$$

and

$$k_>(0,q) = +\frac{1}{2[1+\sin^2\phi\tan^2\theta]} \times\left\{-(-1)^q\left(\frac{h}{2r_0}\right)\sin\phi\tan\theta + \sqrt{\left(\frac{R-r_0}{r_0}\right)^2\left[1+\sin^2\phi\tan^2\theta\right]-\left(\frac{h\sin\theta}{2r_0}\right)^2\cos^2\phi}\right\}, \quad q=1,2. \tag{A.1b}$$

The expression under the radical sign is $\Delta(0,q)$, derived (as a special case) from equation (28). It can be rewritten as

$$\Delta(0,q) = \left\{\left(\frac{R-r_0}{r_0}\right)^2\tan^2\theta\sin^2\phi + \left[\left(\frac{R-r_0}{r_0}\right)^2-\left(\frac{h\sin\theta}{2r_0}\right)^2\right]\cos^2\phi + \left(\frac{R-r_0}{r_0}\right)^2\right\}^{1/2}, \quad q=1,2, \tag{A.2}$$

and due to constraint (5), it satisfies the following inequality:

$$\Delta(0,q) \geqslant \left|\left(\frac{R-r_0}{r_0}\right)\tan\theta\sin\phi\right|, \quad q=1,2. \tag{A.3}$$

Consequently,

$$k_<(0,q) \leqslant 0 \quad \text{and} \quad k_>(0,q) \geqslant 0, \qquad q = 1, 2. \tag{A.4}$$

The above inequalities (A.4) guarantee, according to equation (32b), that $k_{\min}(0,q) \leqslant 0$ and $k_{\max}(0,q) \geqslant 0$. Consequently, according to equations (33)–(35), the range of allowed values of k (corresponding to $\ell = 0$) is not empty, $k = 0$ being necessarily a solution.

Acknowledgement

The programming language *Mathematica* version 3.0.1.1x [23] was used to produce the high resolution graphics presented in this paper. The computations were performed on a 500 MHz Apple Macintosh G4 computer with 1 Gigabit of live memory and 27 Gigabits of hard disk space.

References

[1] J.-J. Max, A.F. Antippa and C. Chapados, Boundary effects in the hexagonal packing of rod-like molecules inside a right circular cylindrical domain. I. The case of right circular spherocylindrical molecules, J. Math. Chem. 21 (1997) 339–358.
[2] A.F. Antippa, J.-J. Max and C. Chapados, Boundary effects in the hexagonal packing of rod-like molecules inside a right circular cylindrical domain. II. The case of inclined spherocylindrical molecules, J. Math. Chem. 24 (1998) 79–108.
[3] A. Ulman, *An Introduction to Ultrathin Organic Films from Langmuir–Blodgett to Self-Assembly* (Academic Press, Boston, 1991).
[4] H.M. McConnell, L.K. Tamm and R. Weis, Periodic structure in lipid monolayer phase transitions, Proc. Natl. Acad. Sci. USA (1984) 3249–3253.
[5] D.P. Parazak, J.Y.-J. Uang, S.A. Whitt and K.J. Stine, Fluorescence microscopy observations of domain structures in Langmuir monolayers of N-stearoylserine methyl ester and N-stearoylvaline at intermediate enantiomeric compositions, Chem. Phys. Lipids 75 (1995) 155–162.
[6] S.W. Hui, R. Viswanathan, J.A. Zasadzinski and J.N. Israelachvili, The structure and stability of phospholipid bilayers by atomic force microscopy, Biophys. J. 68 (1995) 171–178.
[7] D.K. Schwartz, J. Garnaes, R. Viswanathan and J.A.N. Zasadzinski, Surface order and stability of Langmuir–Blodgett films, Science 257 (1992) 508–511.
[8] D.K. Schwartz, M.-W. Tsao and C.M. Knobler, Domain morphology in a two-dimensional anisotropic mesophase: Cusps and boojum textures in a Langmuir monolayer, J. Chem. Phys. 101 (1994) 8258–8261.
[9] M.N.G. de Mul and J.A. Mann, Jr., Determination of the thickness and optical properties of a Langmuir film from the domain morphology by Brewster angle microscopy, Langmuir 14 (1998) 2455–2466.
[10] X.-M. Yang, D. Xiao, S.-J. Xiao, Z.-H. Lu and Y. Wei, Observation of chiral domain morphology in a phospholipid Langmuir–Blodgett monolayer by atomic force microscopy, Phys. Lett. A 193 (1994) 195–198.
[11] J.A. Zasadzinski, R. Viswanathan, L. Madsen, J. Garnaes and D.K. Schwartz, Langmuir–Blodgett films, Science 263 (1994) 1726–1733.
[12] H.M. McConnell, Structures and transitions in lipid monolayers at the air–water interface, Annu. Rev. Phys. Chem. 42 (1991) 171–195.

[13] A.F. Antippa, Tilting operator for phospholipidic molecular domains at the liquid–gas interface, J. Math. Chem. 26 (1999) 179–196.
[14] M. Banville and A. Caillé, Anisotropic molecules forming a monomolecular layer on a strongly adhesive substrate: a scaled particle treatment, Can. J. Phys. 61 (1983) 1592–1598.
[15] D. den Engelsen and B. de Koning, Ellipsometric study of organic monolayers. Part 1. Condensed monolayers, J. Chem. Soc. Farad. Trans. I 70 (1974) 1603–1614.
[16] L. Pauling and R. Hayward, *The Architecture of Molecules* (W.H. Freeman, 1964) Table of bonded atoms and plate 17.
[17] W.T. Lippincott, A.B. Garret and F.H. Verhoek, *Chemistry* (Wiley, 1977) p. 646.
[18] L. Pauling, *The Nature of Chemical Bond* (Cornell University Press, 1960) p. 114.
[19] P. Dutta, J.B. Peng, B. Lin, J.B. Ketterson, M. Prahash, P. Georgopoulos and S. Ehrlich, X-ray diffraction studies of organic monolayers on the surface of water, Phys. Rev. Lett. 58 (1987) 2228–2231.
[20] K. Kjaer, J. Als-Nielsen, C.A. Helm, P. Tippman-Krayer and H. Möhwald, Synchrotron X-ray diffraction and reflection studies of arachidic acid monolayers at the air–water interface, J. Phys. Chem. 93 (1989) 3200–3206.
[21] C.M. Knobler, Seeing phenomena in flatland: studies of monolayers by fluorescence microscopy, Science 249 (1990) 870–874.
[22] B.A. Pethica, M. Glasser and J. Mingin, Intermolecular forces in monolayers and air/water interfaces, J. Colloid. Interface Sci. 81 (1981) 41–51.
[23] S. Wolfram, *Mathematica* (Cambridge University Press, 1996).